Contents

CHAPTER 1: INTRODUCTION

1.1 BACKGROUND OF STUDY AND PROBLEM STATEMENT

Throughout research done, the accuracy of pore pressure prediction is critical in drilling engineering to ensure safety, economically and efficiency drill the well in order to produce gas or oil from reservoir. In real reserve there are normal pressure, abnormal pressure and also subnormal pressure which varies accordingly to the change in formations of well as it is almost impossible to have a well with simple formation characteristics. These change in pressure might also resulted from faults, salt domes, anticline formations and other reasons.

Fracture gradients and pore pressure frequently control well design and also the impact well cost. The depth of casing settings, mud weight, well design and other elements will be relying on accurate assessment of expected pore pressure and fracture gradients.The project will provide guidelines to pore prediction method by trying to be more specific on how the applicability of Eaton's method affected by the properties of the formation. Sensitivity of application of Eaton method affected by the properties of formation especially in fine sediment with shale region as a case study.Pore pressure prediction can be grouped in three categories (David Watson et al, 2003) which are:

(1) Those relied on in planning well
(2) Those can be applied while drilling
(3) After the fact techniques

This study is to access well result after drilling as guideline for future operations.As known, the first all categories are the most important to the design and operational of a drilling project. However, there are certain limitations which the data need to be renewed subsequently after the drilling operations started. Therefore, it is important to have the most reliable source at the first place so that we can reduce the risk relying on every stage of work and automatically reduce the time and cost.

1.2 OBJECTIVE AND SCOPE OF STUDY

The main objectives of the research are to:

1) Analyze the sensitivity of Eaton's pressure prediction method in fine sediments using data manipulation and correlations.

2) Calculate constant for modified Eaton's exponent.

3) Compute the observed pore pressure with normal compaction pore pressure determined.

4) Recommend the applicability of result.

Shale and sandstone formation in BTY 1 will be the study case and different log will be taken as project data such as Gamma ray log, density log, resistivity log and sonic log. Other data required also will be history of well, depth, pressure, temperature, velocity, hydrostatic pressure, density and porosity.

1.3 PROJECT RELEVANCY

The project is very relevant to be continued and can be further implementation by using the project method is recommended especially for students who need a practical solution and application to estimate pore pressure. It is very practical to be used as one of research method due to its feasibility. Kick (Sclumberger, 2012) caused by the pressure in wellbore being less than that of the formation fluids, thus causing flow into the reservoir. Therefore, to overcome this scenario, mud weight must be increased so that hydrostatic pressure exerted on the formation by the fluid column may be sufficient to hold the formation fluid in the formation.

The importance of pressure detection for drilling engineers are also envelops in well strategic planning which with the accurate pore pressure, casing and cement design

basically determined using the mud window. Furthermore, drilling fluid program such as mud, spacer and slurry can be calculated and to prevent loss circulation and formation damage. Thus, rig and equipment selection plus the well architecture also be designed using the pressure obtained.

1.4 PROJECT FEASIBILITY

1.4.1 Feasibility of time

The project will be divided into two parts which is in FYP 1 and also FYP 2 timeline. The amount of time of 30 weeks will be almost sufficient to carry out the studies even though the time is not focusing on FYP project only but also major subjects in course. However, the project hopefully can be completed within the time frame.

1.4.2 Feasibility of research reference

The main equation and principal used in this research is a new findings by (Ebrom et al, 2003) and (Alan R. Huffman, 2011) which are derived primarily from (Eaton, 1975). Plus, the modified Eaton equation is widely used in pore pressure prediction all around the world.

CHAPTER 2: LITERATURE REVIEW AND THEORY

2.1 LITERATURE REVIEW

2.1.1 Recent Advances in Pore Pressure Prediction in Complex Geologic Environments ,2011

The paper discussed on the new technologies used to estimate the pore pressure in complex geologic environment. Usual approach will use time-migrated gathers with well logs and borehole geophysical data from local well control which need details on velocity analysis of the seismic gathers, conditioning well data, calibrating seismic and prediction data. Other data such as overburden is obtained by density log data in order to get vertical stress versus depth relationship referenced to the mud line or land surface.The equations used to obtained the data (Alan R. Huffman, 2011) is vertical stress equals to coefficient a times Z (depth) by b exponent. Calibrations for velocity effective stress also used the power law relationship between velocity and effective stress. The approach taken is good approach as it is proven to be effectively used worldwide. Other famous method used is by Terzaghi's (Terzaghi.K, 1943) basic relationship of ;

Vertical stress = Fluid pressure + Effective pressure

Other conventional approach is using Matthews and Kelly (Matthews.KT, John Kelly, 1967) approach of determining fracture pressure using the equation ;Pf= Pp +K(OB -Pp)

The new method approach of this paper using residual velocity analysis using an AVO phase mismatch methodology had resulted in more accurate pore pressure prediction. This is because well monitoring during drilling using conventional data types such as mud weight, rate of penetration, gas and other was confirmed to be too high in the research because of the presence of open fractures which may resulted in

lost circulation. However, if the new method of using shale velocity data by enhancing and manipulating lost circulation can be prevented.

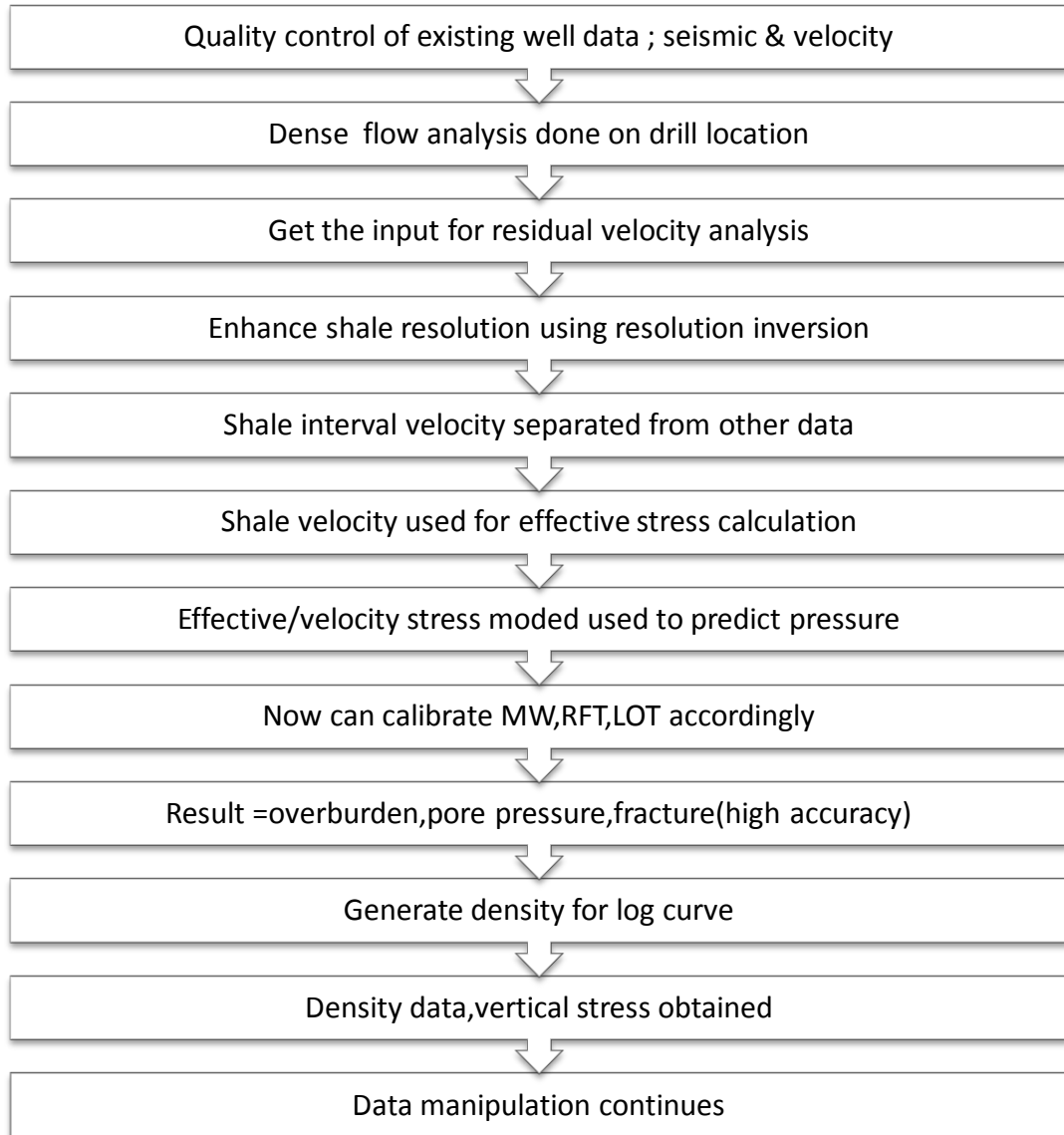| Quality control of existing well data ; seismic & velocity |
| --- |
| Dense flow analysis done on drill location |
| Get the input for residual velocity analysis |
| Enhance shale resolution using resolution inversion |
| Shale interval velocity separated from other data |
| Shale velocity used for effective stress calculation |
| Effective/velocity stress moded used to predict pressure |
| Now can calibrate MW,RFT,LOT accordingly |
| Result =overburden,pore pressure,fracture(high accuracy) |
| Generate density for log curve |
| Density data,vertical stress obtained |
| Data manipulation continues |

Figure 1: Pore Pressure Prediction Method in Complex Geologic Environment (Alan R. Huffman, 2011)

2.1.2   Pore Pressure Prediction based on High Resolution Velocity Inversion in Carbonate Rocks, Offshore Sirte Basin –Libya ,2010

At 72nd EAGE Conference & Exhibition, Barcelona (Javier Buitrago, 2010) had performed geopressure prediction on Sirte Basin, offshore Libya. They had prediction on fluid and fracture pressure based on well control and interval velocities. Using REVEL^{TM} software, this research had used a quite similar method to the one that will be used later on 2011 by Alan R. Huffman (Alan R. Huffman, 2011) which had become an apprentice to them.

Two reservoir-specific pore pressure models with different saturating fluids were generated to take into account for buoyancy effects for prediction of reservoir pressure and seal failure. From down dip pressures P-Max is calculated to a maximum extent of the possible fluid column to predict for pore fill columns using the local closure and spill points and pressure prediction at the penetration point for the reservoir assuming the existence of a centroid equilibrium pressure point in a is a step-like fold in rock strata consisting of a zone of steeper dip within an otherwise horizontal or gently-dipping sequence.

The input data gathers and velocity field was to produce an inverted velocity cube . The shale velocities was calibrated to get effective stress in 3D.Other data produced was pore pressure (PP),pore pressure gradient(PPG), overburden pressure (OB),overburden pressure gradient (OPG), fracture pressure (FP) and fracture pressure gradient (FPG).

The conference also reviewed on well monitoring and post well. They found out that the Eaton method that was originally applicable for the Gulf of Mexico shows the method cannot be applied on the latest carbonate base (Javier Buitrago, 2010) . Thus, the Bower's method (Bowers, 1995) are likely become more suitable.

The limitations of Eaton and D-exponent are they strongly dependent on shale compaction data and cannot reliably calibrate in present carbonate setting. The conference had listed 8 requirements for successful predictions (Javier Buitrago, 2010).
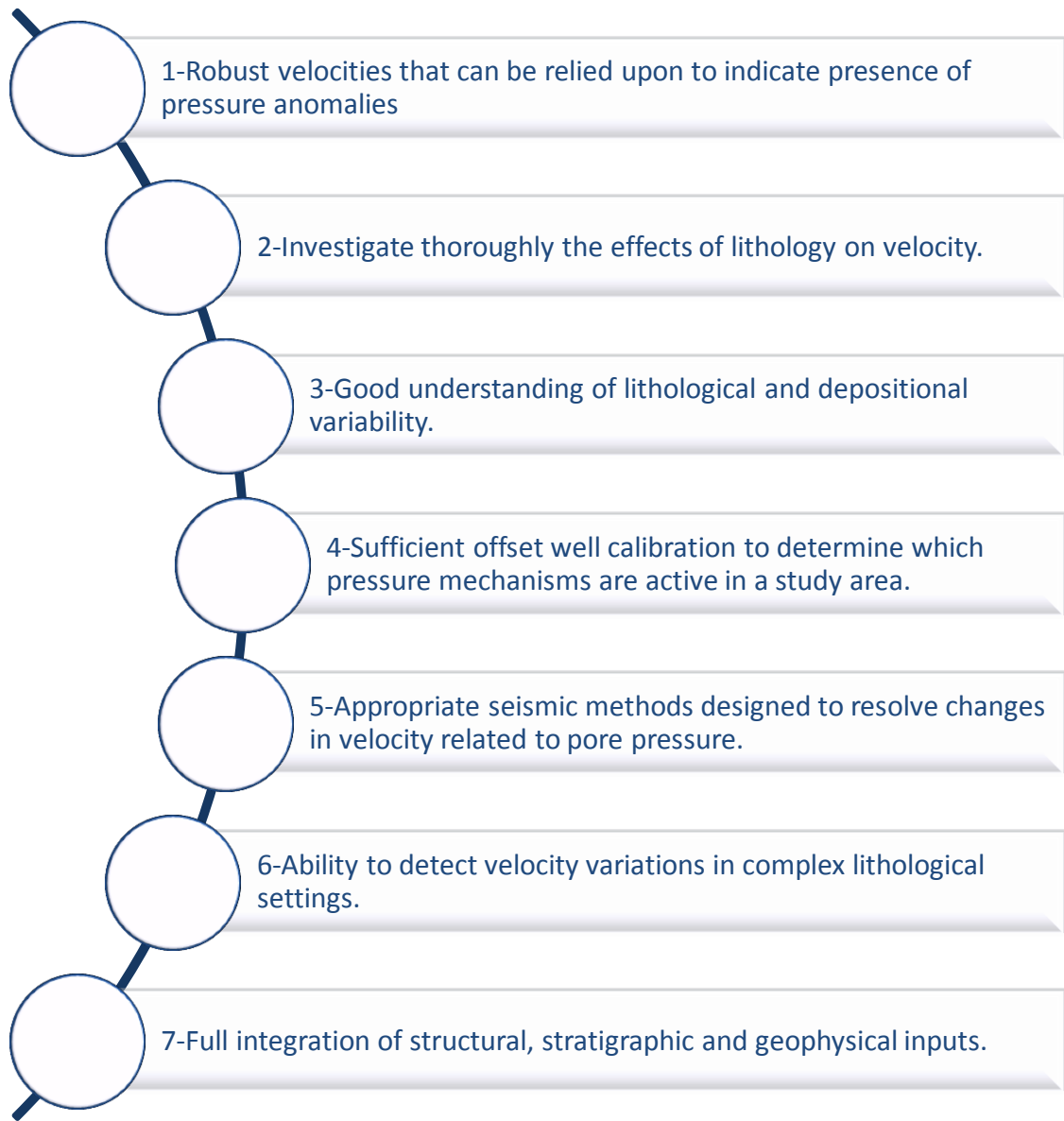
List of 8 Requirements for successful drilling;

1-Robust velocities that can be relied upon to indicate presence of pressure anomalies

2-Investigate thoroughly the effects of lithology on velocity.

3-Good understanding of lithological and depositional variability.

4-Sufficient offset well calibration to determine which pressure mechanisms are active in a study area.

5-Appropriate seismic methods designed to resolve changes in velocity related to pore pressure.

6-Ability to detect velocity variations in complex lithological settings.

7-Full integration of structural, stratigraphic and geophysical inputs.

Figure 2: Requirement List for Successful Drilling

The conclusions that can be described on this paper review are that it is the beginning of new approach by obtaining pressure data by using the shale velocities.

2.1.3 Estimation of Pore Pressure from Well logs: A theoretical analysis and Case Study from an Offshore Basin, North Sea (Vera, 2010)

In this pore pressure estimation , Miller's sonic equation had been used (Miller, 1995) to determine pore pressure from four deep water wells. The major concern at this case study is the pore pressure gradients because it is the main guide for development of mud schedule ,casing programme , rig selection and wellhead ratings.

Using the mud windows authors tried to describe the relationship among casing setting depth ,formation pore pressure gradient and fracture gradient in figure1 (Sarker.R, 2010). Sonic travel time of sediment at mud line is obtained by extrapolating the normal compaction curve to mud line.

If the data points exist is higher than the virgin curve (Vera, 2010) ,unloading can be inferred. The results of research are overburden gradient (OBG) is dependent on the water column where if we have a higher water column, the OBG will be lower and vice versa. The other finding by author is normally the normal pore pressure will increase with depth.
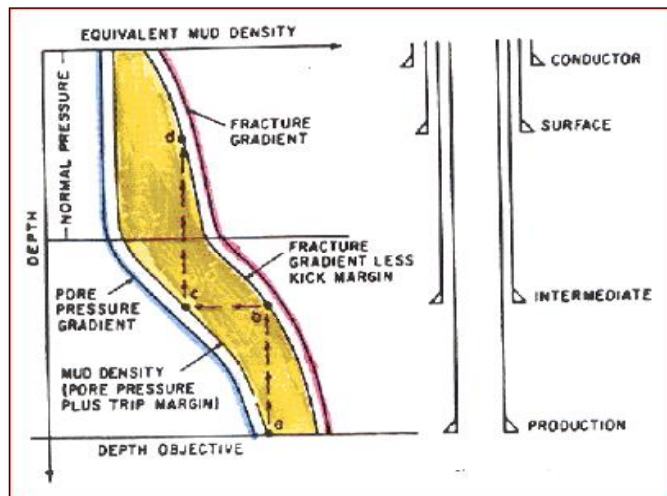

Figure 3: Mud Window (Sarker.R, 2010)[10]

2.1.4 Pore pressure prediction using an Eaton's approach for PS-waves (Kimberly M.Kumar, 2006)

The research study is on the effect of shallow gas will result in poor seismic quality and velocity for P-waves. Therefore Kumar and their team will used a modified Eaton's approach for pressure prediction using PS-waves move out velocities.

The P-wave velocity deviation was first used by (Hottman & Johnson, June 1965) and (Pennebaker Jr, June 1968) from normal compaction trend to detect pore pressure and estimate pressure using empirical calibration curves. The findings once again discussed on Eaton's method (Eaton, 1975) which said that the ratio of P-wave velocity obtained from regions of normal and abnormal pressure is relate to ratio of normal and abnormal pressure where the exponent can be determined empirically (Eaton, 1975).

The limitations of method are he exponential is general to Gulf of Mexico only and can't be reliable in overpressure regions associated with high porosity and high gas content. This is due that the high gas content can deteriorate the P-wave reflections.

Eaton's where restricted to P-wave analysis in gas saturated media and S-wave is more suitable to use as it is independent of bulk modulus, therefore the gas has no effect on S-wave energy and sensitive to gas saturation. Thus this resulted in reliability of pressure predictions (Ebrom et al, 2003) .

According to research, direct comparison between sonic derived velocities and seismically derived velocities shows that shallow gas decelerates P-wave velocities but for PS-wave, it is less affected. To conclude, the Eaton method can be modifies successfully for PS-wave and PS-wave is most effective method to map overpressure region. Reliable source also directs to correct calibration of mud weight.

2.1.5   Brief: Pore and Fracture Pressure Determinations: Effective Stress

According to the research, lithology and porosity are the main input required to calculate overburden and effective stress. The other input data from wire line such as gamma ray, density , resistivity and sonic also useful to get pore pressure and fracture pressure. The deviation of results of using input data of lithology and porosity compared to repeat formation leak off test is small which is between 0.06 g/cm^3 and 0.04 g/cm^3 (Ward et al, Brief: Pore and Fracture Pressure Determinations: Effective Stress, 1995). The assumptions used for the method is rock has no tensile strength.

2.2 THEORITICAL VIEW

2.2.1   Shale Properties, Origin and Behavioral

Shale properties are determined by the fine grain size of the individual minerals. The mineralogy of shale is very variable which the average shale contains quartz and other forms of silica, feldspars and carbonate mineral such as calcite and dolomite with addition of iron oxide and dolomite. Some of shale are detrital, but digenetic and others have in-situ and volcanic varieties.

The formation of fine grained sediments like shale will only require weak transporting currents of other transporting methods such as winds and turbidity. Most shale can be found in environment like the deep ocean, continental slope and rise, seas, bays, lagoon, deltas and also river flood plains. Shale has its own economic value as black shale can become the sources of petroleum products and metals. (Britannica, 2012)

As the time passes, mud that been deposited layered by other sediments such as sandstone on top. The deposition of new layers can reach thousands of feet above the original layer. Therefore, the pressure beyond will increase and compaction in mud occur. The compaction will expel the remaining fluid inside mud and physically changed the clay particle to be slit like as the pressure is in vertical direction.

With stable compaction of layer and overburden stress applied gradually in thousands of year, normal pore pressure might be obtain as the pore fluid can be expel continuously. Pore pressure usually increase due to increasing in depth. However this can be changed if during the burial and compaction overpressure occurs. Overpressure occurs when burial is so rapid and permeability is so poor that the pore fluid cannot escape and supports ever-increasing stress resulting different pressure gradient in affected area which caused both fluid and shale will have to support the overburden pressure.

2.2.2   Loading Mechanisms

Loading curve can be obtained by using log effective stress, Mpa versus log solidity (1-ɵ) (Ward et al, Brief: Pore and Fracture Pressure Determinations: Effective Stress, 1995). The graph shows that the porosity decrease while effective stress will gradually increase with loading. The curve means that the sediment burial consolidation path is normal where full fluid escape happen along with increasing of overburden load (Ward et al, Brief: Pore and Fracture Pressure Determinations: Effective Stress, 1995).In this case, the effective stress will increase while porosity decrease and pore pressure become hydrostatic.

However, if the fluid is restricted to escape, porosity and effective stress will become constant. The constant effective stress may result in pore pressure increase in the same rate as overburden pressure and finally develop overpressure. This mechanism is called under compaction or compaction disequilibrium.

2.2.3   Unloading Due Fluid Expansion or Charging

Fluid expansion or charging mechanism unload the sediment and can be observed through velocity and porosity. Fluid expansion mechanism such as organic maturation and cracking aqua thermal expansion, and mineral digenesis can all charge fluid pressure within the pore space. Fluid expansion mechanism requires a very low permeability seal and suitable temperature conditions to become important (Ward et al, Brief: Pore and Fracture Pressure Determinations: Effective Stress, 1995).

This mechanism will create extreme overpressures which approach or even exceed fracture gradient. Basins will become shallower with increasing temperature gradient. It suggests that overpressures are temperature related phenomena through mechanism such as hydrocarbon generation, clay mineral digenesis and aqua thermal pressuring.

2.2.4   Pore Pressure Prediction Methods

The approach of the compaction methods is to measure porosity indicators in normally pressured shale and establish a normal compaction trend with depth. In order to obtain accurate results, measurement should be taken in clean shale or shale with minimum of other rock mixtures.

Equivalent Depth Method (Osegoei, 2011)

As compaction is not effective in abnormal trend zone, the porosity should be deviated from the normal trend line. By using equivalent depth method, every data point in the under compacted region has counterpart in the normally pressured section, given by the equation:

$$Pp = Pn(eq) + [\sigma ob - \sigma ob(eq)]$$

Where $\sigma ob(eq)$ and $Pn(eq)$ = overburden stress and pore pressure at the equivalent depth.

D-Exponent (Adam T.Bourgoyne et al, 1986)

The d-exponent equation can be used to detect the transition from normal to abnormal pressure if the drilling fluid density is held constant. The technique involve is plotting values of d obtained in a given type of low permeability formation as a function of depth. In normally pressure formation, d-exponent tends to increase with depth.

Dexp=[log(R/60N)]/[log (12W/1000db)]   (Jorden and Shirley 1996)

Plotting the graph D vs D exp

Gp=Gn (D normal/D observed)   (Zamora et al)

Eaton's Method (David Watson et al, 2003)

Eaton's empirical equation that do incorporate the overburden gradient. Below relationships are widely used for the log-derived methods, conductivity data plots, resistivity and many more.

$$Gp = Gop - (Gob - Gn)\left(\frac{\Delta Tn}{\Delta To}\right)^{\wedge}3* \qquad Gp = Gop - (Gob - Gn)\left(\frac{\Delta Ro}{\Delta Rn}\right)^{\wedge}1.2*$$

$$Gp = Gop - (Gob - Gn)\left(\frac{\Delta Cn}{\Delta Co}\right)^{\wedge}3 *$$

*c=3.0 if transient time data available while c=1.2 if shale resistivity data available.

Wyllie's Time Average (Jack Dvorkin et al, 2001)

$$\tau_{p=}\tau_{S+}\tau_{F} \qquad\qquad\qquad (1)$$

$$\frac{1}{Vp} = \frac{1-\emptyset}{Vps} + \frac{\emptyset}{VpF} \qquad\qquad (2)$$

Above are expressions that relate velocity to porosity and to pore-fluid compressibility while the slowing express velocity to porosity transformation.

$$V_p = (1 - \emptyset)^2 V_{pS} + \emptyset V_{pF,} \quad \emptyset < 0.37 \qquad\qquad \text{(Raymer et al, 1980)}$$

$$\rho = 0.23 V_p^{0.25} \qquad\qquad \text{(Gardner et al, 1974)}$$

$$\rho = (1 - \emptyset)\rho_s + \emptyset\rho_F \qquad\qquad \text{(Gardner et al, 1974)}$$

$$V_p = [\frac{(1-\emptyset)\rho_s + \rho_F}{0.23}]^4 \qquad\qquad \text{(Gardner et al, 1974)}$$

Modified Eaton

$$\left(\frac{\sigma_o}{\sigma_n}\right) = \left(\frac{V_{po}}{V_{pn}}\right)^{Ep} \qquad\qquad \text{(Jeff Kao at al, 2010)}$$

Vpo are the interval velocities observed in Malay basin field under abnormally pressured conditions. $V_{pn,}$ are the interval velocities in normally pressured environments. Hamilton and Eberhart-Phillips velocities are used as V_{po} inputs. σ_o are predicted effective stress values that are solved for when all other inputs are satisfied. σ_n are effective stress value in a normally pressured region. Eps is an empirically determined Eaton's PS-wave exponent.
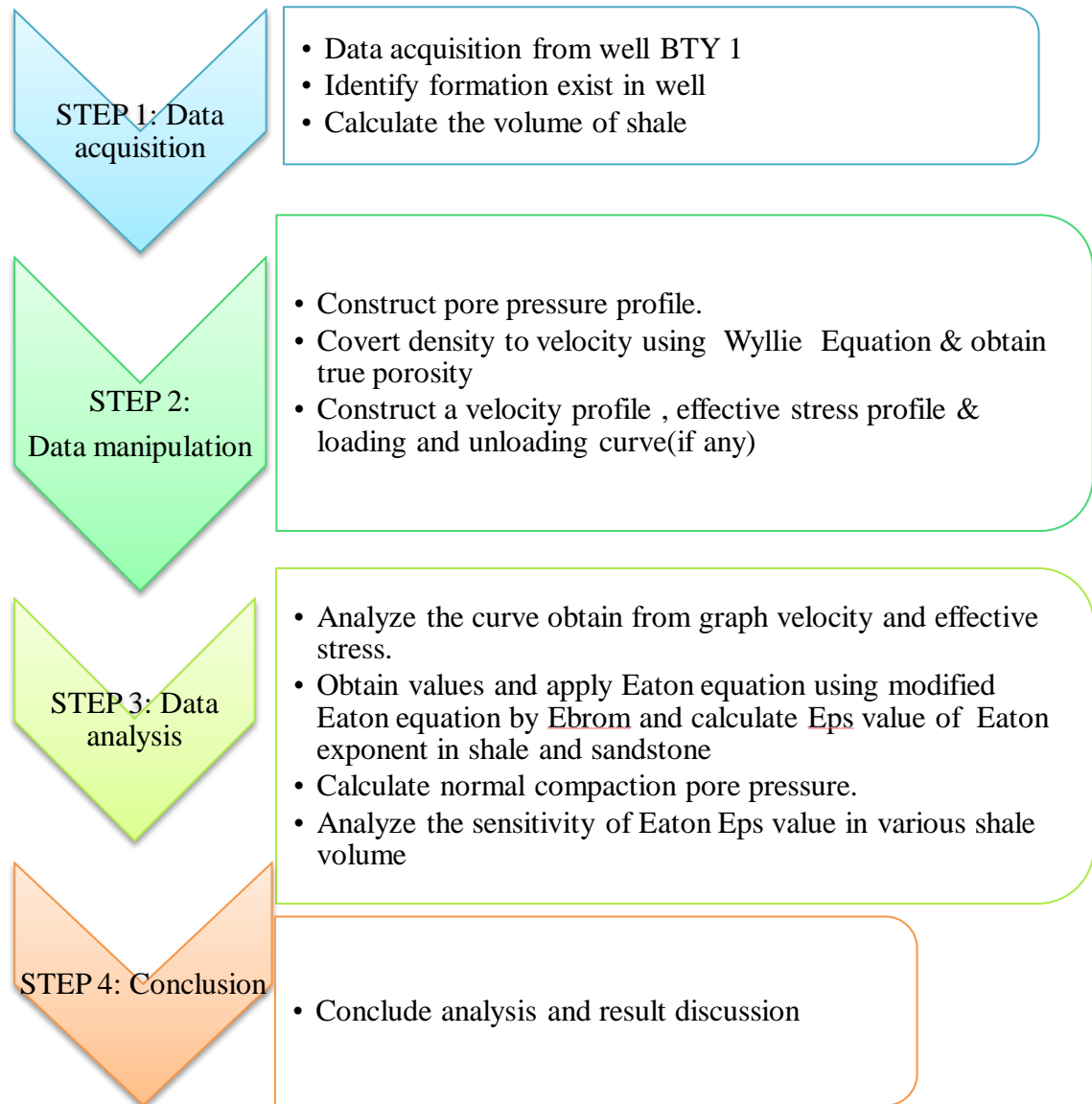
CHAPTER 3: METHODOLOGY

3.1 RESEARCH METHODOLOGY

STEP 1: Data acquisition
- Data acquisition from well BTY 1
- Identify formation exist in well
- Calculate the volume of shale

STEP 2: Data manipulation
- Construct pore pressure profile.
- Covert density to velocity using Wyllie Equation & obtain true porosity
- Construct a velocity profile , effective stress profile & loading and unloading curve(if any)

STEP 3: Data analysis
- Analyze the curve obtain from graph velocity and effective stress.
- Obtain values and apply Eaton equation using modified Eaton equation by Ebrom and calculate Eps value of Eaton exponent in shale and sandstone
- Calculate normal compaction pore pressure.
- Analyze the sensitivity of Eaton Eps value in various shale volume

STEP 4: Conclusion
- Conclude analysis and result discussion

Figure 4: Proposed Methodolgy for Pore Pressure Prediction

3.2 PROJECT ACTIVITIES
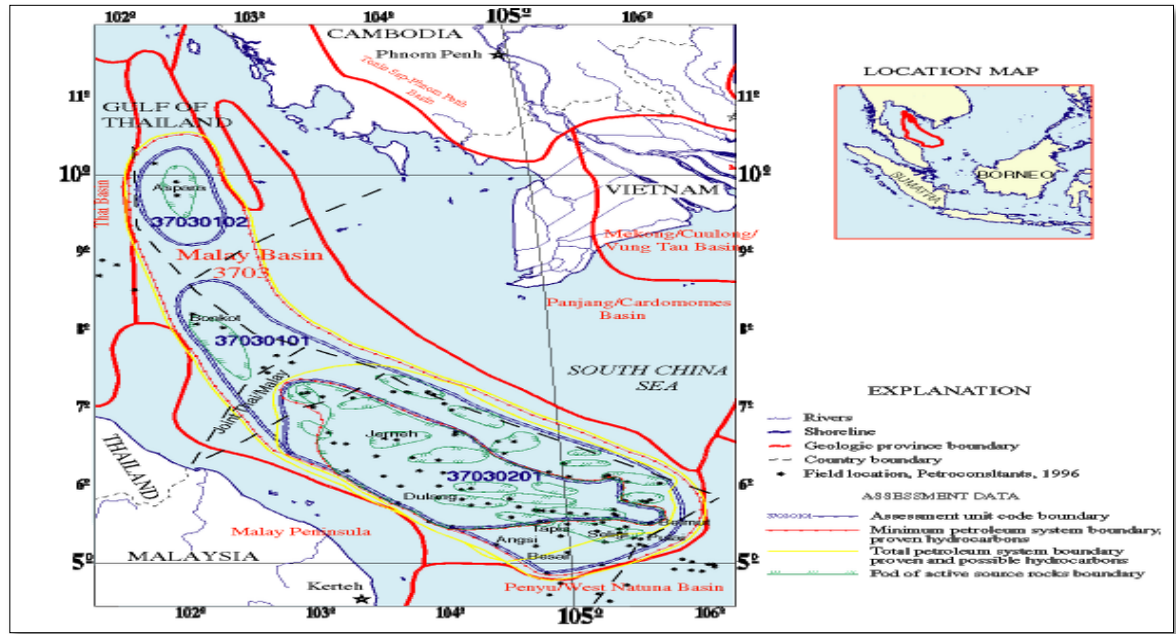
Step 1:Data acquisition

Figure 5: Malay Basin (G.Bishop, 2002)

The Malay Basin Province is located offshore line and composed of the Malay Basin (primarily in the waters of Malaysia, with smaller portions in the waters of Thailand, Indonesia and Vietnam) and the Khmer Trough (in Cambodian waters).Water depth is less than 200 m. The province has produced more than 1.6 billion barrels of oil (Petro Consultants, 1996).The research data is obtain from an example well of BTY 1, located in Malay basin. The basic data input provided are density porosity, neutron porosity, depth, permeability, lithostatic pressure, volume of shale, formation velocity, porosity and temperature. Malay basin is also infamously known of its capable of having oil and gas fields that mostly located at the southwestern part. Sandstone of Late Oligocene to Middle Miocene age produce oil and gas from its formation along other factors with suitable structural trap had captured oil and gas from further migrate to other places. Using well logging, basic data is acquired from well BTY 1 and be used as default data for research.

Step 2: Data Manipulation
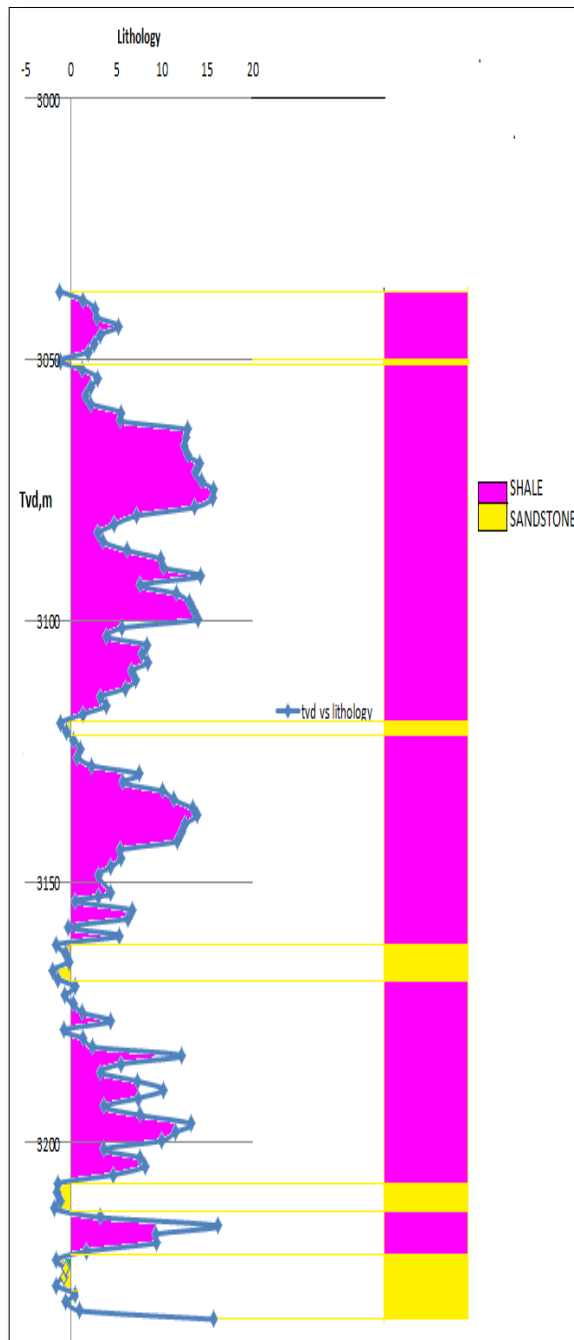
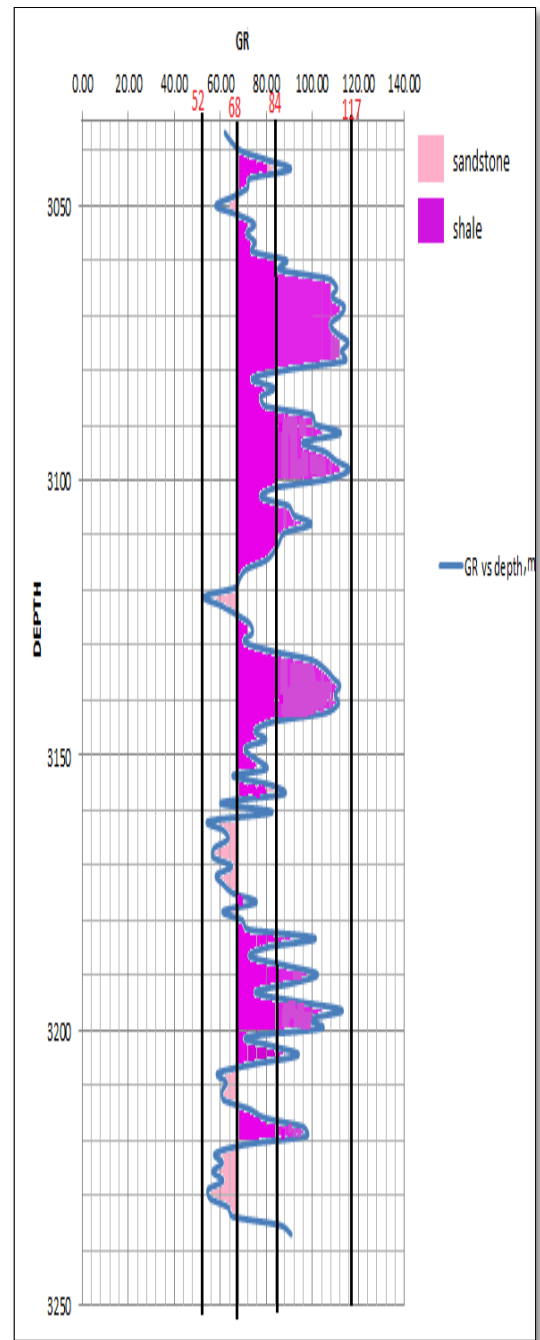Construction of type of formation graphs:

Figure 6: GR vs Tvd

Figure 7: Lithology vs Tvd

Construction of shale volume and pore pressure graphs :
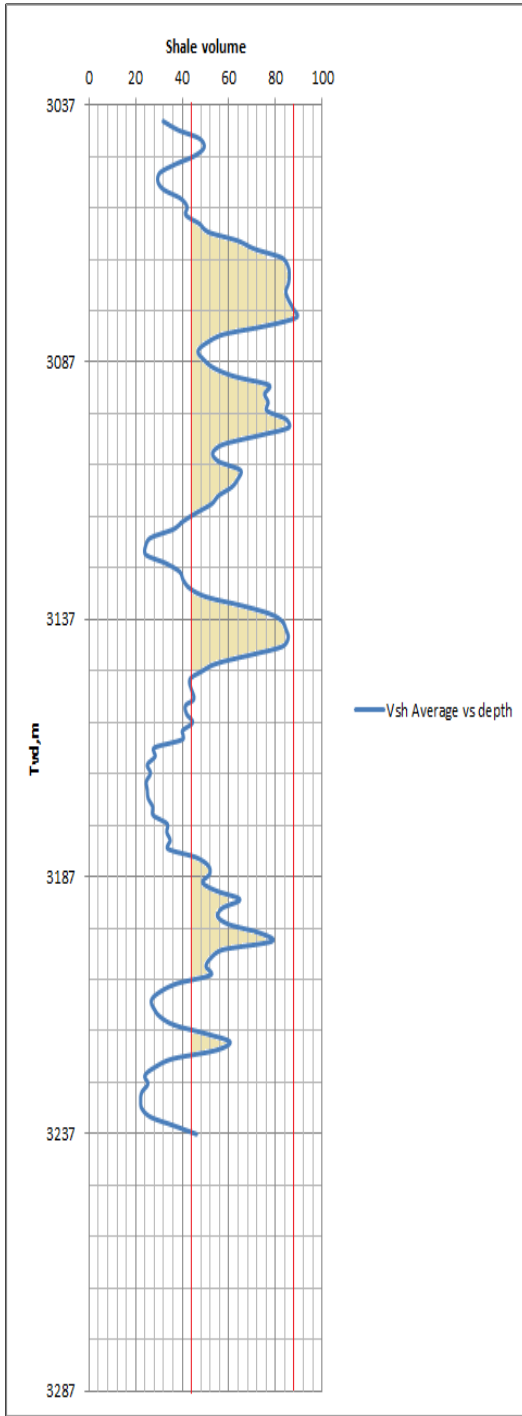

Figure 8: Vshale average vs Tvd

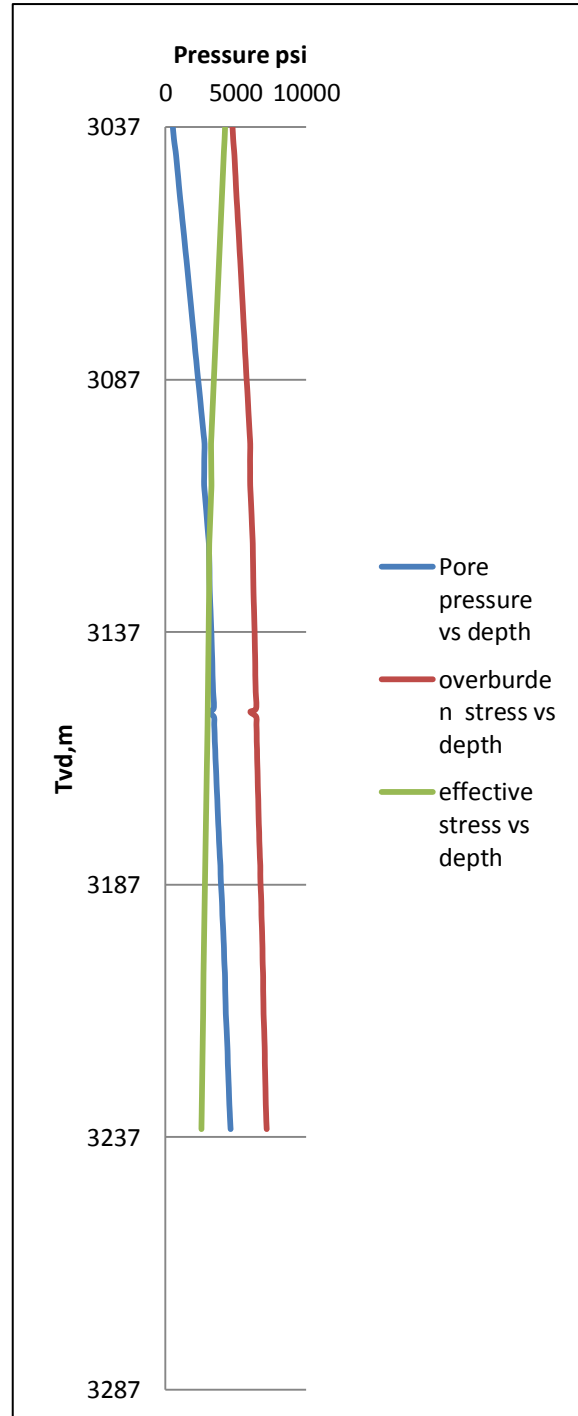**Figure 9: Various pressure vs Tvd**

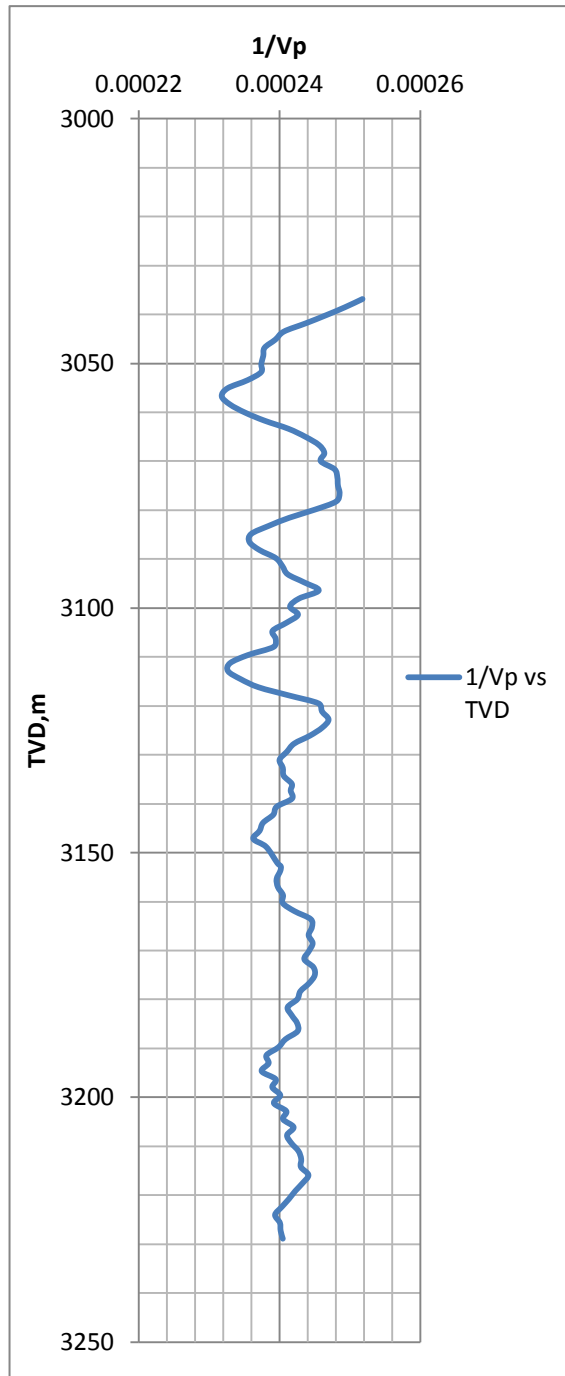Construction of type of 1/Vp and neutron density porosity graphs :
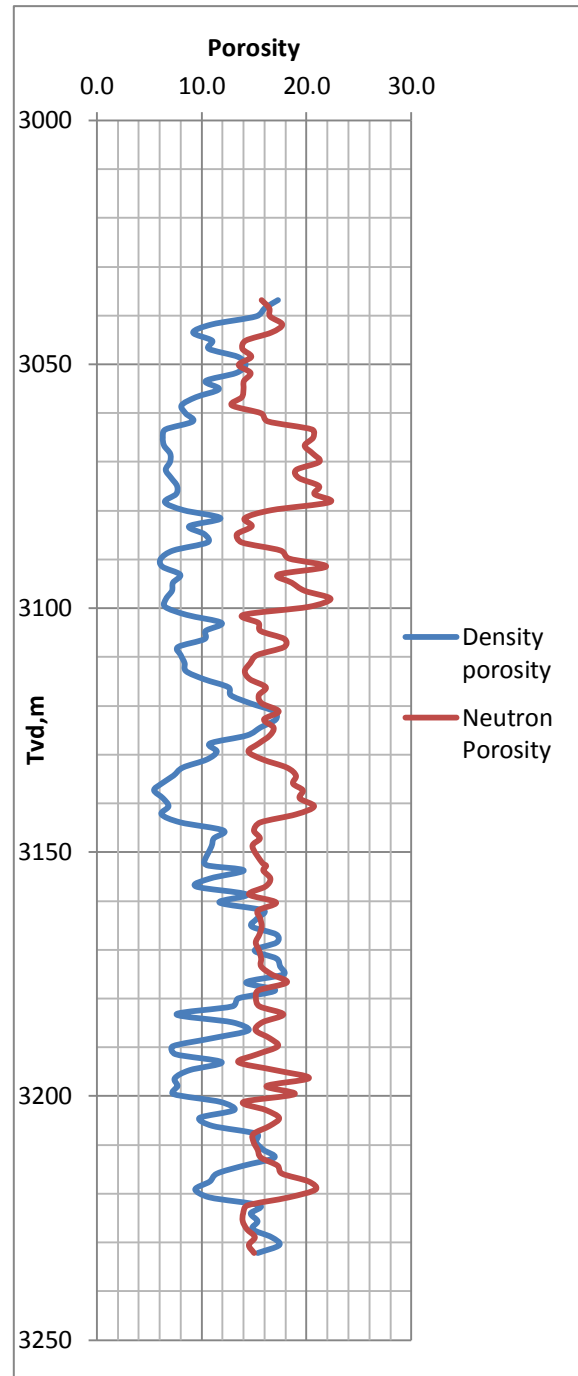

Figure 10: 1/ Vp vs Tvd

Figure 11:Porosity log

3.4 KEY MILESTONE

No	Detail/Week	1	2	3	4	5	6	7	8	9	10	11	12	13
1	Complete activities 1 , 2 , 3 & 4	▨	▨	▨	▨	▨	▨	▨						
2	Further discussion							▨	▨	▨	▨	▨	▨	

3.5 GANTT CHART

FYP1

No	Detail/Week	1	2	3	4	5	6	7	8	9	10	11	12	13
1	Topic Selection/Proposal	▨	▨					▨						
2	Preliminary Research Work		▨	▨	▨	▨		▨						
3	Submission of Proposal Defense Report						▨	▨						
4	Proposal Defense (Oral Presentation)							▨	▨	▨				
5	Data acquisition and pre-predictions							▨			▨	▨	▨	
6	Preliminary conclusions							▨			▨	▨	▨	
7	Submission of Interim Draft Report							▨					▨	
8	Submission of Interim Report							▨						▨

▨	Work completed
▨	Submission Due
▨	In progress
▨	Mid Term Holiday
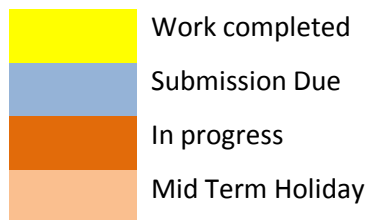
FYP 2

No	Detail/Week	1	2	3	4	5	6	7	8	9	10	11	12	13	14	15
1	Project work continues	▓	▓	▓	▓	▓	▓	█								
2	Submission of progress report							█	▒							
3	Project work continues							█		▓	▓	▓	▓			
4	Pre-EDX							█				▒				
5	Submission of draft report							█					▒			
6	Submission of dissertation							█						▒		
7	Submission of technical paper							█						▒		
8	Oral presentation							█							▒	
9	Submission of project dissertation							█								▒

▓ Process

▒ Submission Due

█ Mid Term Holiday

3.6 HARDWARE AND TOOLS

This project will not intend to use any kind of software to develop programming or simulating the data. However, spreadsheet is needed in order to accumulate all the field data and some part of calculations will be generated the formula here. Briefly, from this project, it is essential to estimate pore pressure, given effective stress and velocity thus, the following general procedure is recommended:

1. Examine the historical data, rejecting both anomalously low value and/or anomalously high value in situation such as:

2. Well logging data

3. Regress the remaining data with the rate/time equation that results in the "best" fit

Up to this, these are what generally can be executed from this project; nevertheless, the method will be added, changed and eliminated due to some circumstances later on.

CHAPTER 4: RESULT AND DISCUSSION

4.1 DISCUSSION

4.1.1 Pore Pressure

1. Pore pressure

    Observed pressure test is measured in sand. Prediction of pressure used in shale

2. Overburden stress

    Overburden stress is defined as the pressure exerted by the weight of the overlying sediments. The overburden load is supported by the vertical stress in the grain framework and by the fluid pore pressures.

3. Figure 9 shows the pore pressure increase with the increase of overburden pressure. The gap between these two pressures indicate the effective stress. As the depth go deeper, effective stress decrease from 4300 psi to 2600 psi. The trend is similar to Jincai Zhang's prediction that stated effective stress will continuously decrease until it almost approach to the overburden stress,Therefore, the trendline stated in figure 9 is absolute normal trends.
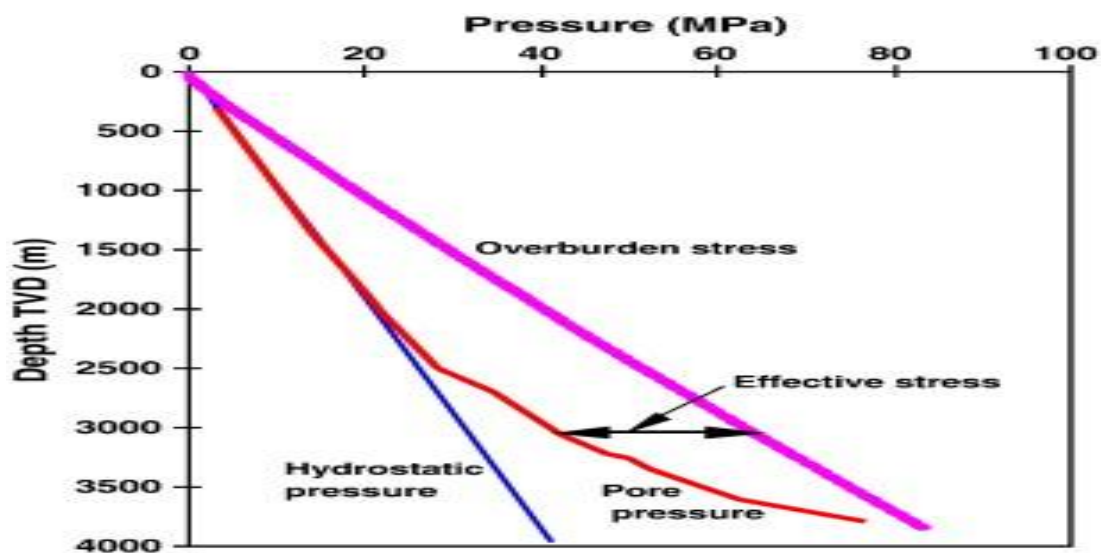
Jincai Zhang,2011

4.1.2 Fine Sediment

1. Correlation figure 7 suggested that the composition of the formation is mainly shale due to high GR value in MeV stated in base data well of BTY1 while the volume of sandstone is low. This result is also supported by other data from the well which stated that lithology indicator will mark negative value for sandstone and positive value for shale as in figure 6.

2. According to Crain's Petro physical handbook

Crain's Rule #0: Gamma ray or SP deflections to the left indicate cleaner sands, deflections to the right are shaly. Draw clean and shale lines, then interpolate linearly between clean and shale lines to visually estimate Shale Volume (Vsh).

3. The well formation was determined by constructing simple graph using the Gamma Ray versus depth. Gamma ray log uses radioactivity which result in decay of an unstable nucleus through emissions of particles energy. It has photons, high frequency electromagnetic energy travelling at light speed (PETRONAS, 2008). For average values of drilling mud and formation density, we can say that roughly 50% of the gamma ray signal originates from inside 18 cm (7 inches) of the borehole wall, increasing to 75% from within 30 cm (1 foot).

Hence, the depth of study, if defined at 75% of the signal, is 30 cm. Though, this will drop for denser formations of the similar radioactivity, and upsurge for less dense formations of the same radioactivity. Clean sandstone or limestone has low GR reading while shale and clay formations will have a high GR reading. It is assumed that the shale formation can be obtained by using below equation.

$$\text{Clean Shale} = \frac{\text{GRmax}-\text{GRmin}}{2} \quad \text{if GR} > 80$$

Shale volume computation can be calculated using below equation.0.49 or 49% are shale volume.

$$\text{Vshale} = \frac{\text{GRlog} - \text{GRmin}}{\text{GRmax} - \text{GRmin}}$$

GR =   Gamma ray log reading in zone of interest   ,   =84

GR min =   Gamma ray log reading in 100% clean zone   ,   =52

GR max =   Gamma ray log reading in 100% shale   ,   =117

Gamma Ray log can have been affected by cave in or cave out along borehole and also barite drilling muds. However, corrections can be made using Gamma Ray log correction chart by Reeves Wireline Ltd at certain depth where caving can be detected using caliper log during determination of the borehole size.

4. Calculation of average shale volume is an adaption of equation of modified harmonic permeability average (Infohost, 2012) equation using the shale volume in the spreadsheet (Appendix I). It is assumed that shale region is when Vsh > 44.This method is used in order to have a smooth shale volume. As the depth increased, the volume of shale began to deplete and the highest depletion rate is at depth 3125 m with shale volume average of 25.

5.

$$V_{\text{sh,avg}} = \frac{\sum_{i=1}^{N} H}{\sum_{i}^{N} H/Vsh}$$

H=   Depth, m

Vsh=   Volume at shale at the depth

6. Figure 9 shows an early prediction where overburden pressure is higher than observed pore pressure.

7. The combination of density and neutron logs is now used commonly as a means to determine porosity that is largely free of lithology effects. Each individual log records an apparent porosity that is only true when the zone lithology matches that used by the logging engineer to scale the log. A limestone-equivalent porosity is a good choice for both neutron and density logs, because calcite has properties that are intermediate between dolomite and quartz.

    According to the porosity log in figure 11,the neutron and density porosity log had overlapping between the depth of 3160 m and 3180 m (butterfly effect) which possibility to have presence of hydrocarbon which is possible to have because it is positioned in the sandstone lithology that is known as a reservoir rock.Density porosity gives the indication of what type of HC. Gas has low density compare to crude. Neutron on the other hand give us how porous is the formation. When we bombard the for formation with hydrogen. If the formation is sand, we will have a low neutron reading while if it shale high return hydrogen readings.

8. By averaging the apparent neutron and density porosities of a zone, effects of dolomite and quartz tend to cancel out. The true porosity may be estimate either by taking an average of the two log readings or by applying the equation:

$$\emptyset = \sqrt{\frac{\emptyset_n^2 + \emptyset_d^2}{2}}$$

    Where $\emptyset n$ and $\emptyset d$ are neutron and density porosities. It has been suggested that the square-root equation is preferable as a means of suppressing the effects of any residual gas in the flushed zone.

    The obtain porosity using the equation above had resulted in almost linear porosity profile. This is because the depth of investigation is in the unloading region where the porosity had become linear instead of decreasing with depth (Appendix 2). The compaction of lithology is no longer applicable in this region because water prevents formation from further compacted.

With this finding, we can assume that later on we will find differences in normal compaction pore pressure compared to the observed pore pressure as presented early in figure 9.
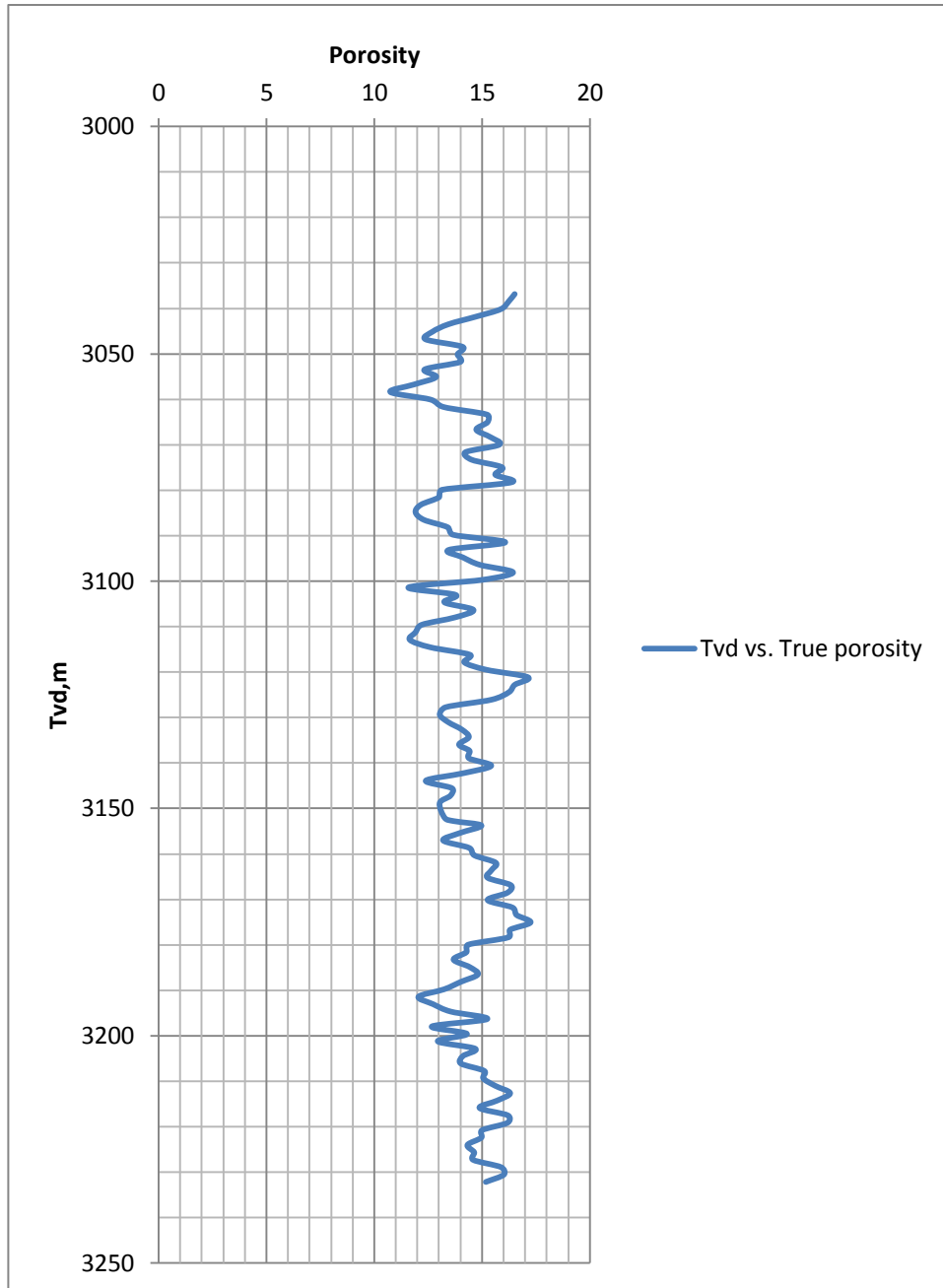
Figure 12: True porosity vs Tvd

9. Wyllie time average state $\dfrac{1}{Vp} = \dfrac{1-\emptyset}{Vps} + \dfrac{\emptyset}{VpF}$, hence the result will be as figure 10.

1/Vp is the transit time use in sonic or acoustic log measures the travel time of an elastic wave through the formation. This info can also be used to derive the velocity of elastic waves through the formation. Its main use is to provide information to support and calibrate seismic data and to derive the porosity

of a formation.

The main uses are (Glover, 2012):

- Provision of a record of "seismic" velocity and travel time throughout a borehole. This information can be used to calibrate a seismic data set (i.e., tie it in to measured values of seismic velocity).

- Provision of "seismic" data for the use in creating synthetic seismograms.

- Determination of porosity (together with the FDC and CNL tools).

- Stratigraphic correlation.

- Identification of lithologies.

- Facies recognition.

- Fracture identification.

- Identification of compaction.

- Identification of over-pressures.

- Identification of source rocks

In figure 10, the average transit time decrease with increase in depth. The gas has low density, therefore it decrease the apparent density of the formation. This proves the butterfly effect region (3160 m to 3180 m) is a sandstone formation that caused 1/Vp has become lower (Appendix 3).

4.1.3 Modified Eaton:

$$\left(\frac{\sigma_o}{\sigma_n}\right) = \left(\frac{V_{po}}{V_{pn}}\right)^{Ep}$$

1. History and Elaboration of Formula

    Eaton's (1969) equation for estimating pore pressure trends from seismic velocities is applied using observed PS-wave velocity values obtained from six nodes in Atlantis Field. Eaton's method relates pore pressure to deviations in Pwave velocity from an established depth trend.

    As inputs to Eaton's equation, Hamilton (1972, 1976) and Eberhart Phillips et al. (1989) regressions are used to represent velocities in a normally pressured marine environment. An effective stress gradient is modeled for a normally pressured zone, and Eaton's exponent is set to a value between 2.6 as a base point for computation. Ebrom et al. (2003) incorporate S-wave velocities from multicomponent surveys into a modified Eaton's equation for pore pressure prediction.

2. Figure 9 shows that the effective stress decreases as depth increase. Increase of depth meaning that the burial also increases. The phenomenon was resulted from overpressure in fluid expansion, and then the pore pressure will upsurge at faster rate. Under compaction only cannot cause the effective stress to decrease. Fluids within the clay-bearing rocks cannot escape due to their very low permeability. During burial, increasing overburden pressure is the prime cause of fluid expulsion. If the sedimentation rate is slow, normal compaction occurs, i.e., equilibrium between increasing overburden and the reduction of pore fluid volume due to compaction (or ability to expel fluids) is maintained (Mouchet and Mitchell, 1989).

3. This normal compaction generates hydrostatic pore pressure in the formation. Rapid burial, however, leads to faster expulsion of fluids in response to rapidly increasing overburden stress. When the sediments subside rapidly, or the formation has extremely low permeability, fluids in the sediments can only be partially expelled. The remained fluid in the

pores of the sediments must support all or part of the weight of overly sediments, causing the pressure of pore fluid increases, i.e., abnormally high pore pressure. In this case porosity decreases less rapidly than it should be with depth, and formations are said to be under-compacted or in compaction disequilibrium.

4. Using graph in figure 13, 14, 15 and 16, all the variables will be obtain. There are two types of formation exist, therefore the modified Eaton equation will be applied on both shale and sandstone. The Eps value will soon become constant and applicable for reference in pore pressure prediction methods

5. Shale region at depth 3144m.Vpo is equal observed curve of velocity obtained by data log. Vpn is obtained from a straight line correlation of normal curve correlated from the observed curve. Actual normal curve should be gradually increase with increase of depth. However, as the vertical depth investigated is only a small column, assume that it is a straight line and it will not affect much the value.
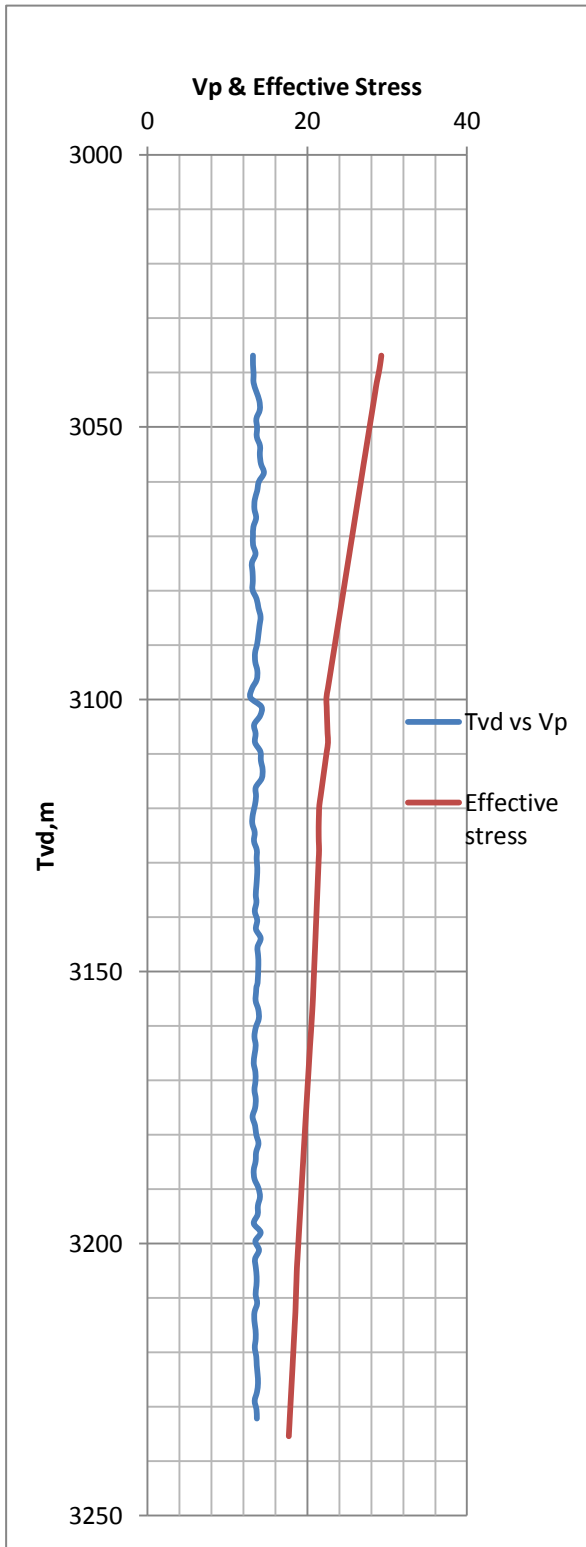
Figure 13: Effective Stress vs Tvd
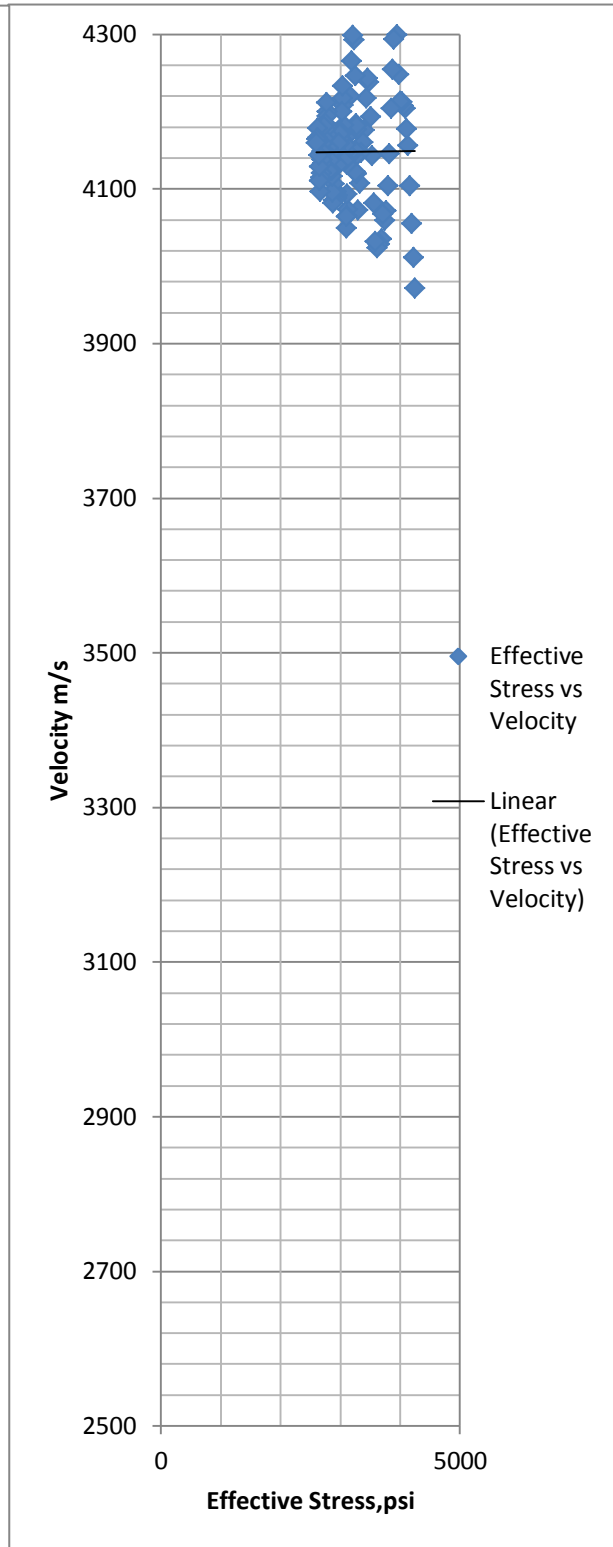
Figure 14: Effective Stress vs Velocity
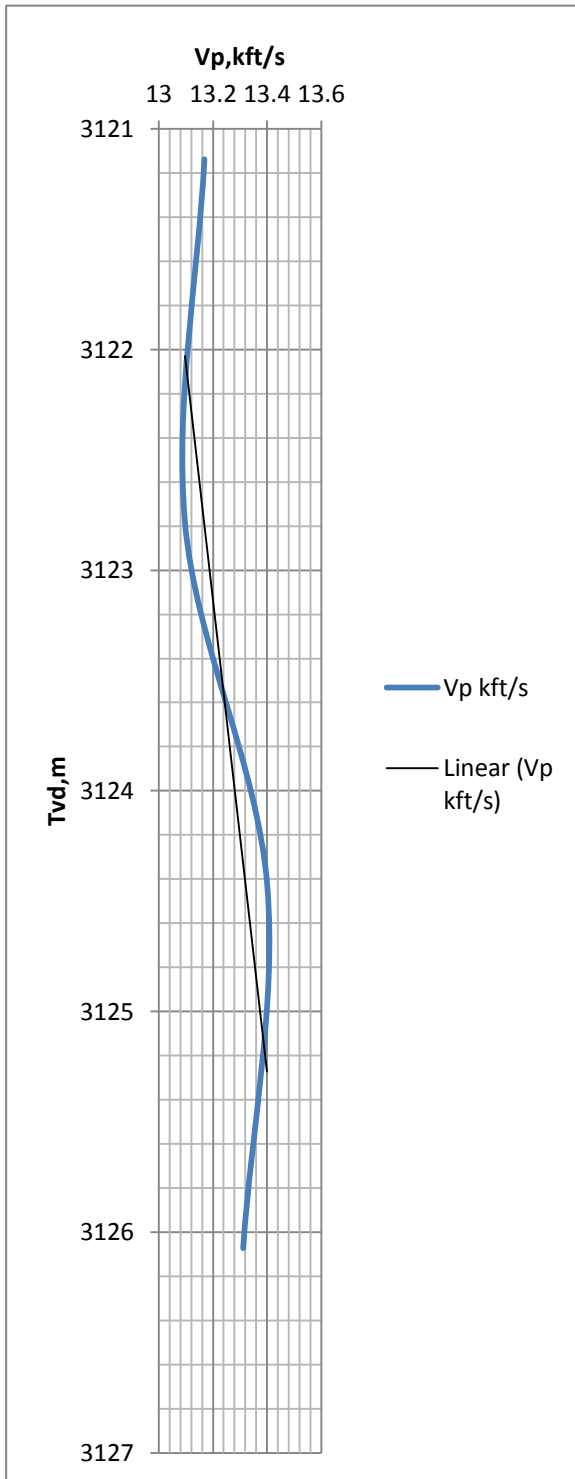
Figure 15: Sandstone Vp vs Tvd
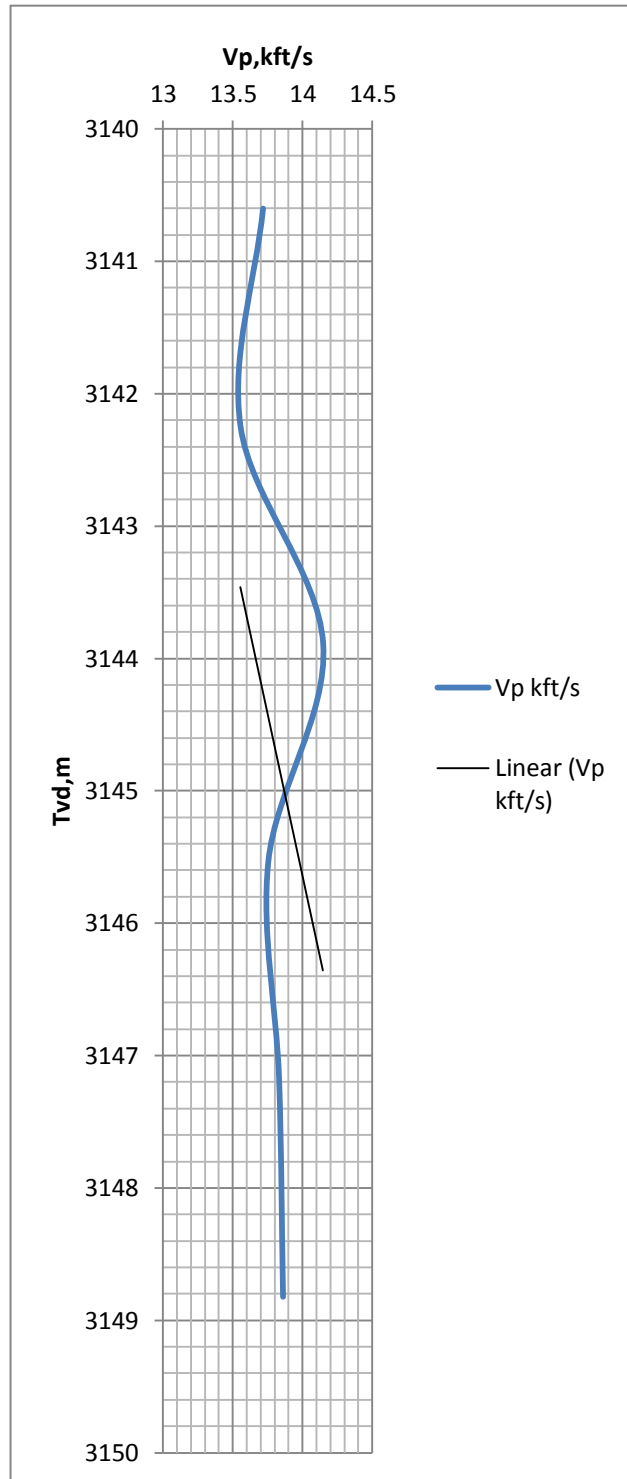
Figure 16: Shale Vp vs Tvd

.

4.2 CALCULATIONS

1.Calculations for shale volume:

$$\text{Vshale} = \frac{\text{GRlog} - \text{GRmin}}{\text{GRmax} - \text{GRmin}}$$

$$\text{Vshale} = \frac{84 - 52}{117 - 52} = 0.4923 \; or \; 49.23\%$$

GR = Gamma ray log reading in zone of interest , =84

GR min = Gamma ray log reading in 100% clean zone , =52

GR max = Gamma ray log reading in 100% shale , =117

2.Calculations for sandstone:

At depth 3123m,

$$\left(\frac{\sigma_o}{\sigma_n}\right) = \left(\frac{V_{po}}{V_{pn}}\right)^{Ep}$$

$$\left| \left(\frac{21.45}{19.90}\right) = \left(\frac{13.12}{13.20}\right)^{Ep} \right|$$

$$\left| log\left(\frac{21.45}{19.90}\right) = log\left(\frac{13.12}{13.20}\right)^{Ep} \right|$$

$$\left| log\left(\frac{21.45}{19.90}\right) = E_p log\left(\frac{13.12}{13.20}\right) \right|$$

$$\left| E_p = -12.34 \right| = 12.34$$

3.Calculations for shale:$\emptyset$

At depth 3144m,

$$\left(\frac{\sigma_o}{\sigma_n}\right) = \left(\frac{V_{po}}{V_{pn}}\right)^{Ep}$$

$$\left| log\left(\frac{21.2}{17.7}\right) = log\left(\frac{14.14}{13.65}\right)^{Ep} \right|$$

$$\left| log\left(\frac{21.2}{17.7}\right) = E_p log\left(\frac{14.14}{13.65}\right) \right|$$

$$\left| E_p = 3.372 \right| = 3.372$$

4. Applying Eps shale = 3.372 in shale region as per predicted in *figure 13*

$$\left(\frac{\sigma_o}{\sigma_n}\right) = \left(\frac{V_{po}}{V_{pn}}\right)^{Ep}$$

$Pp = Poverburden - Effective\ stress$

Values use:

H depth,	$V_{pobserved}$	$V_{pnormal}$	$\sigma_{observed}$	$\sigma\ normal,$ calculate		
				observed	calculated	psi
3141	13.70	13.05	21.10	18.00	17.91	2597.625
3142	13.58	13.25	21.05	17.90	19.37	2809.38
3143	13.85	13.50	21.00	17.80	19.26	2793.426
3144	14.15	13.67	21.00	17.50	18.69	2710.755

Table 1: Effective Stress Calculation

| H depth, | P overburden | P pore pressure,psi | |
	psi	observed	calculated, normal
3141	6366.526	5945.82	3768.901
3142	6381.205	5958.47	3571.825
3143	6385.00	5960.12	3591.574
3144	6389.156	5971.12	3678.401

Table 2:Normal compaction pore pressure calculation
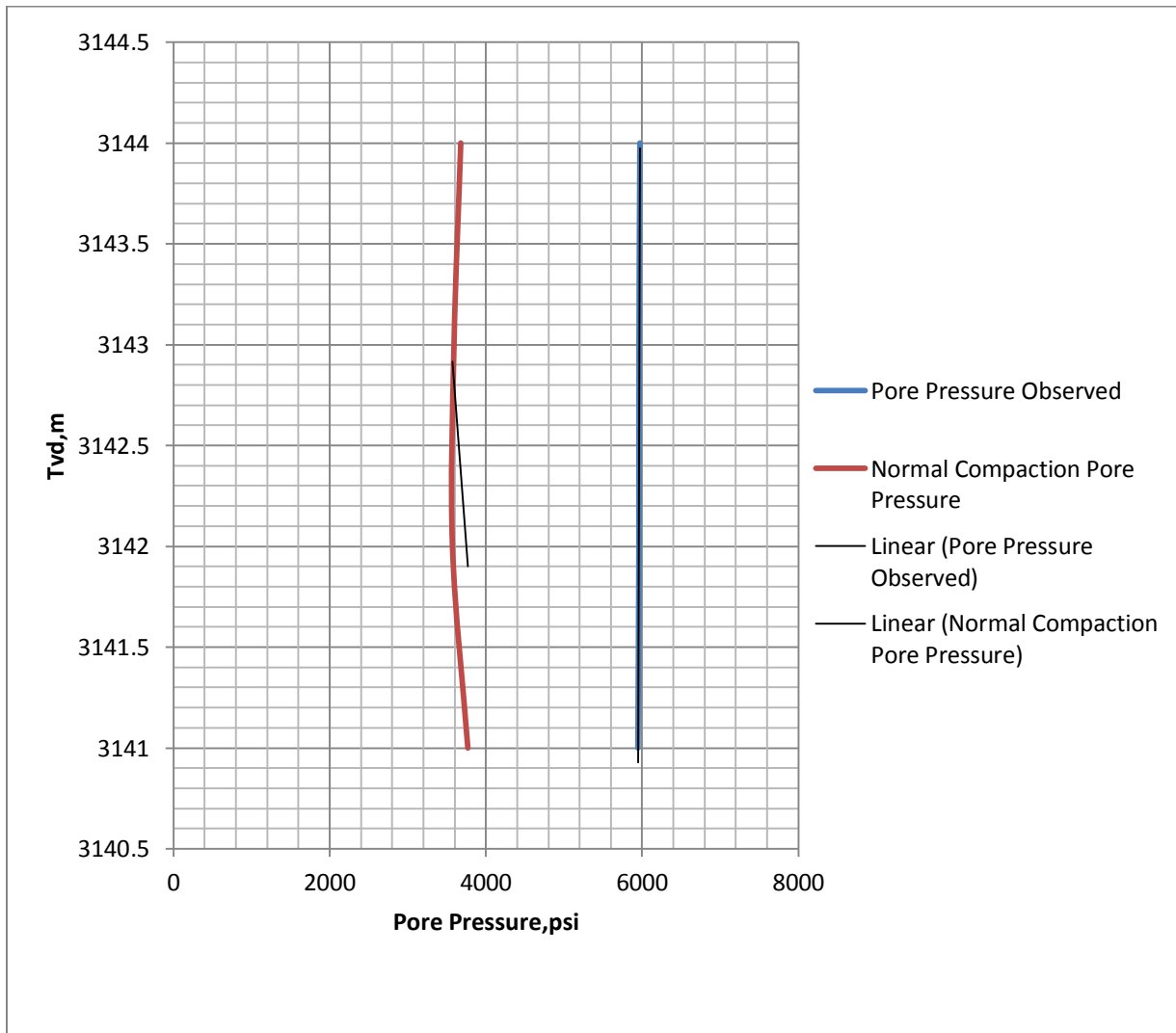
Figure 17: Comparison of pore pressure observed and normal compaction pore pressure calculated using the method approach

Using the approach, the normal compaction pore pressure is lower than the observed pore pressure in figure 9. This means that the shale region between depth 3140 to 3145 (the depth can be extended further until it meets the meeting point of normal compaction and observed pore pressure) is actually in abnormally pressured region.
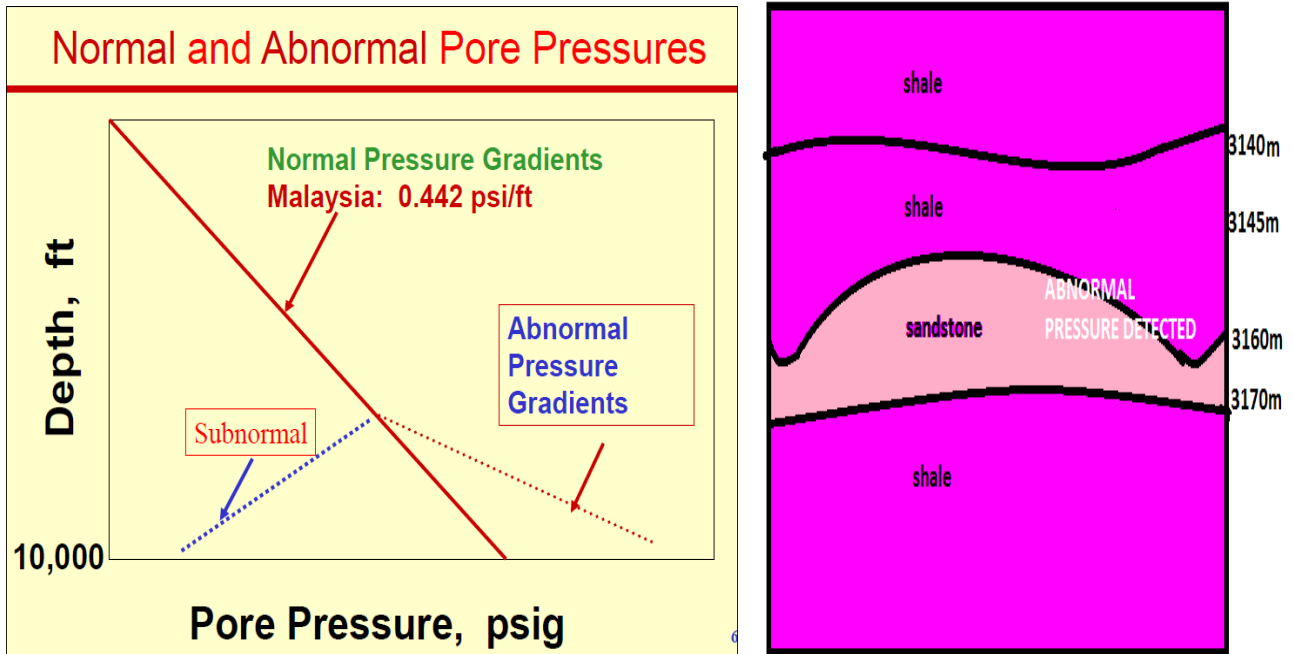
Figure 18: Pore pressure in normal, subnormal and abnormal region (Osegoei, 2011)

Figure 19: Illustration of findings

Abnormal pressure is very dangerous as it can cause severe drilling problem. There are conditions that can cause abnormal pressure occur such as artesian systems, structural reasons, tectonics, surface erosion, rock diagenesis , thermal effects, biochemical effects, osmosis through shale and also external pressure sources man made or naturally occur.

However, the main principle of development of abnormal pressure is it require some means of sealing or trapping the pressure within the rock body which this abnormal pressure found in shale which is a good cap rock to trap the presence of hydrocarbon at depth 3160 to 3170 m (figure 11) above the sandstone (figure 7) also at the same depth. Therefore, we can say that the application is really reliable to be used in fine sediments especially in shale.

5. Sensitivity of Eps value versus Shale Volume

Depth,m(in shale)	Shale Volume	Vp Normal	Vp Obs	Effective stress Normal	Effective stress Obs	Eps
3125	20%	13.14	13.15	22.2	21.4	48.24
3127	40%	13.46	13.54	22.2	21.4	6.19
3132	60%	13.64	13.72	21.8	21.4	0.47
3137	80%	13.90	13.62	21.4	21.2	0.46

Table 3: Determination of Eaton sensitivity
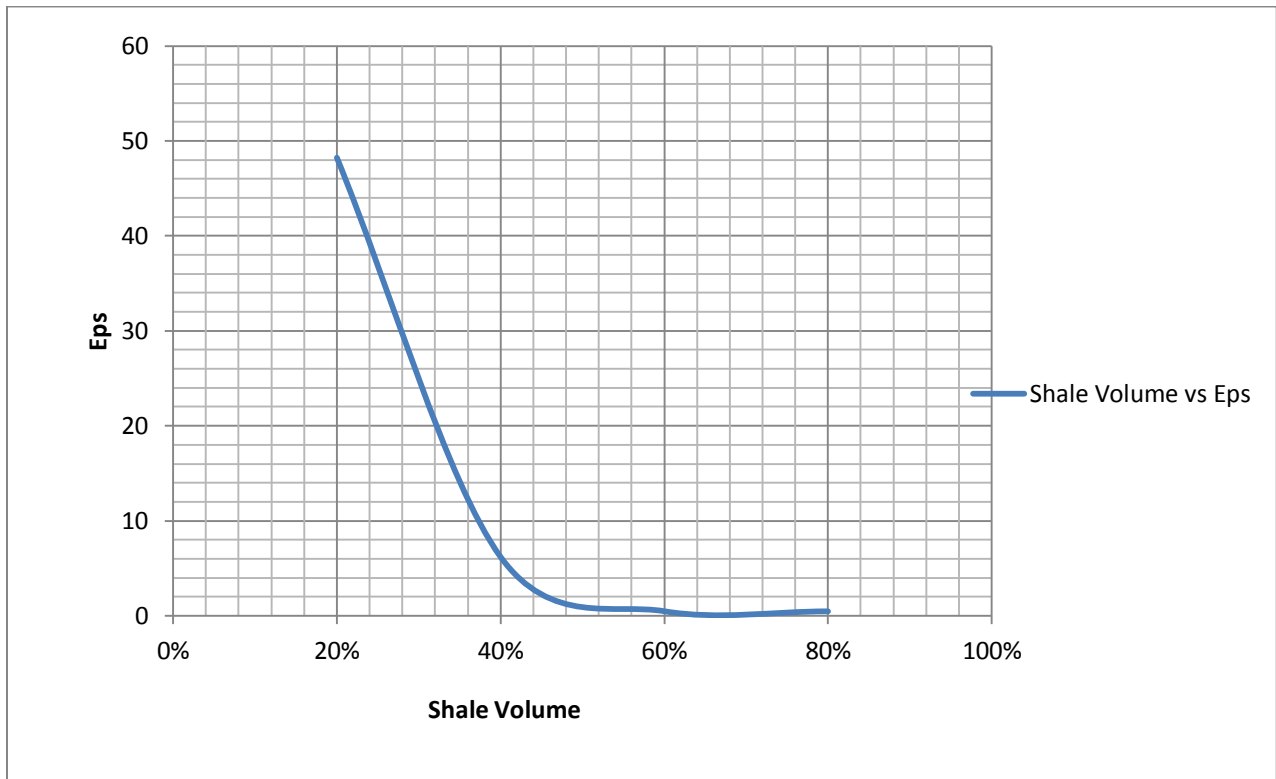
Figure 20: Eps vs Shale Volume

From the figure above we can say that the Eaton exponent Eps more sensitive in high shale volume compared to low shale volume.
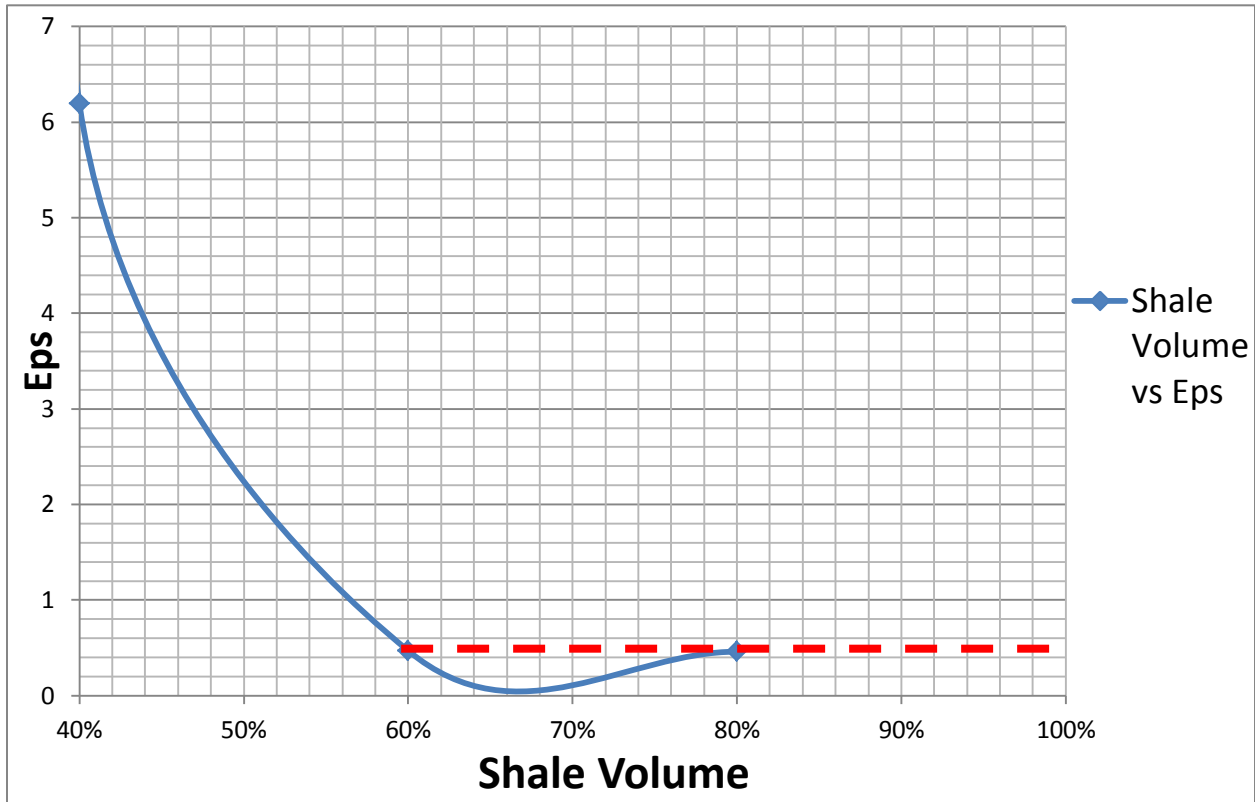
(Above figure is the enlarge figure 20)

The valid value for this correlation is in the assume Vshale which more than 44%. Value of Eaton exponent Ep more smaller in high shale volume compared to low shale volume and above graph can be used as a reference as Ep constant in modified Eaton equation will reflect to volume of shale. The findings is really close to the actual data of Eaton s constant range of 3.0 to 0.33.

The well has primary mechanism of overpressure which is compaction. The graph does not deviate which shows it doesn't have secondary mechanism of pore pressure such as expansion or inflation .Secondary mechanism cannot be evaluate by Eaton because Eaton only applicable for compaction only. Thus, secondary mechanism must use other method.

CHAPTER 5: CONCLUSIONS

The Eps calculated in shale can be used for finding the normal compaction pore pressure in fine sediment . The predicted result will be the Eps value decrease with the increase of shale volume. The Eps value of Eaton exponent versus the volume of shale can be further develop in future research The drillers can detect the change of formation and can be aware of the actual normal compaction pore pressure therefore they can predict the required density of mud weight should be used to prevent incidents such as kick or loss circulation.

.

As a conclusion, this project is a comprehensive research study about application of Eaton method in estimating the pore pressure prediction data and helps improve the pressure prediction especially in shale. Hopefully by using these concepts it becomes possible to provide more accurate production forecasts and better oil and gas reserves for both wells and fields.

Through the discussion before, we can conclude that the method proposed has achieved most of the main objectives of the project which are:

1) Calculate constant for modified Eaton's exponent.
2) Compare the observed pore pressure with normal compaction pore pressure determined.
3) To analyze the sensitivity of Eaton's pressure prediction (Eps) method in fine sediments.
4) Recommend the applicability of result.

RECOMMENDATIONS

The result may be improved by:

   I.   Analysis of more well data

  II.   Analysis of the whole column

 III.   Further study of effect of HC column in pore predictions.

 IV.   Test result in other similar geological set up.

  V.   Use of software to generate graphs.

 VI.   Verification of shale type before applying method:

        a.   Kaolin   :Nactite, Kasolite, Dictite

        b.   Smectite   :Dioctahedral , Triotahedral

        c.   Illite   :Clay micas

        d.   Chloride   :Variety of similar minerals

BIBLIOGRAPHY

Infohost. (2012). Retrieved from faculty: infohost.nmt.edu

Adam T.Bourgoyne et al, K. K. (1986). *Applied Drilling Engineering.* JP.

Alan R. Huffman, J. M. (2011). Recent Advances in Pore Pressure Prediction in Complex Geologic Environment.

Bowers, G. L. (1995). Pore Pressure Estimation From Velocity Data:Accounting For Overpressure Mechanism Besides Under Compaction. *SPE Paper:Exxon Production Research*.

Britannica. (2012, January). *Sedimentary rock*. Retrieved 2012, from Origin of Shale: www.britannica.com

David Watson et al, T. B. (2003). *Advanced Well Control.*

David Watson,Terry Brittenham,Preston L.Moore. (2003). *Advanced Well Control.*

Eaton, B. A. (1975). The Equation for Geopressure Prediction From Well Logs . *SPE 50th Annual Fall Meeting.* SPE.

Ebrom et al, H. P. (2003). Pore Pressure Prediction from S-Wave ,C-wave and P-Wave Velocities. *International Meetings Society of Exploration Geophysics;Expanded Abstracts.*

G.Bishop, M. (2002). *Petroleum Systems of The Malay Basin Province.* Malaysia.

Gardner et al, G. (1974). Formation Velocity and Density:The Diagnostic Basis For Stratigraphic Traps., (pp. 2085-2095).

Glover, D. (2012). *The sonic or acoustic log.* Retrieved April 16 , 2012, from www2.ggl.ulaval.ca

Hottman, C. E., & Johnson, R. K. (June 1965). Estimation of Formation Pressure for Logs Derived Shale Properties . *Journal of Petroleum Technology*.

Jack Dvorkin et al, A. N. (2001). Time Average Equation Revisited. Department of Geophysics Stanford University.

Javier Buitrago, J. D. (2010). Pore Pressure Prediction based on High Resolution Velocity Inversion in Carbonate Rocks. Offshore Sirte Basin-Libya.

Jeff Kao at al, R. H. (2010). Estimating Pore Pressure Using Compressional and Shear Wave Data from Multicomponent Seismic Nodes in Atlantis Field,Gulfwater Mexico. SEG Paper.

Kimberly M.Kumar, D. E. (2006). Pore Pressure Prediction using Eaton's Approach for PS waves. *Jackson School of Geosciences,BP America Exploration and Production Technology Group,Texas.*

Matthews.KT, John Kelly. (1967). Oil and Gas Journal. *How to Predict Formation Pressure and Fracture Gradients*.

Miller, T. (1995). New Insights on NAtural Hydraulic Fractures Induced By Abnormally High Pressure. *AAPG Bulletin*.

Osegoei, D. E. (2011). Advanced Drilling Engineering. *Lecture Notes*. UTP.

Pennebaker Jr, E. S. (June 1968). Seismic Data Indicate Depth MAgnitude of Abnormal Pressure. *World Oil*.

Petro Consultants. (1996). *Petrolem Exploration and Production Database.* Geneva, Switzerland: Petro Consultants.

PETRONAS. (2008). *Well Intervention Seminar.* Malaysia.

Raymer et al, H. E. (1980). An Improved Sonic Transit Time to Porosity Transform. *SPWLA 21 Annual Logging Symposium* , (pp. 1-12).

Sarker.R, B. (2010). *Experimental Verification on the Effects of Effective Stress on Compressional and Shear Wave Velocities in North Sea Shale.* Colorado: Colorado School of Mines.

Sclumberger. (2012). *oilfield glossary*. Retrieved 2012, from www.glossary.oilfield.slb.com.

Terzaghi.K. (1943). *Theoretical Soil Mechanics.* New York: John Wiley & Sons.

Vera, P. (2010). *Estimation of Pore Pressure from Well Logs :A Theoretical Analysis and Case Study from Offshore Well Basin.* Hydrabad.

Ward et al, K. C. (1995). *The Journal of Petroleum Technology,SPE*.

Ward et al, K. C. (1995). Brief: Pore and Fracture Pressure Determinations: Effective Stress. *The Journal of Petroleum Technology,SPE*.

Jincai Zhang, Pore pressure prediction from well logs: Methods, modifications, and new approaches for http://www.sciencedirect.com , 2011.

Jeff Kao, Estimating Pore Pressure Using Compressional and Shear Wave Data from Multicomponent Seismic Nodes in Atlantis Field, Deepwater Gulf of Mexico, SEG Annual Meeting ,2010

APPENDICES

Appendix 1:Basic data spreadsheet from well BTY 1(AP Wan Ismail Wan Yusoff)

0.442		max	123.55		Density	Neutron	Apparent	Pressure	Effective	Vp	Fluid	Litho indicator
pore pressure	TVDmss	GR	Vsh	RHOBC	porosity	Porosity	Permeability	Mpa	Stress	m/sec	Indicator	
1379.543	3121	52.90	18	2.41	16.9	17	1.75	40	21	4015	0.37	0.43
1427.175	3229	54.56	20	2.41	16.7	15	1.51	46	18	4085	0.43	-1.58
1397.579	3162	54.83	20	2.42	15.9	15	0.98	42	20	4075	0.53	-0.53
1427.894	3231	55.57	21	2.40	17.4		2.32	46	18	4155	0.44	
1425.737	3226	56.58	22	2.43	15.3	14	0.70	46	18	4212	0.55	-1.41
1400.479	3169	56.85	22	2.40	17.2	15	2.01	43	20	4112	0.83	-1.99
1399.754	3167	57.24	23	2.40	17.1	16	1.98	43	20	4047	0.63	-1.62
1424.298	3222	57.65	23	2.43	15.5	14	0.79	46	18	4164	0.32	-1.17
1348.15	3050	57.91	24	2.45	14.2	14	0.36	32	28	4177	0.46	-0.66
1401.929	3172	58.16	24	2.40	17.1	16	1.97	43	20	4076	0.55	-1.45
1417.815	3208	58.87	25	2.44	15.3	15	0.67	45	19	4152	1.43	-0.32
1396.129	3159	60.02	26	2.45	14.3	15	0.38	42	21	4244	0.70	0.24
1380.27	3123	60.44	27	2.41	17.1	16	1.92	40	21	3993	0.35	-1.13
1419.256	3211	60.74	27	2.43	15.9	15	0.96	45	19	4180	1.72	-0.54
1425.018	3224	60.97	27	2.45	14.7	14	0.48	46	18	4195	0.41	-0.72
1404.822	3178	61.07	27	2.41	17.0	15	1.85	43	20	4099	0.65	-1.61
1426.456	3227	61.19	27	2.44	14.8	14	0.53	46	18	4173	0.48	-0.53
1398.304	3164	61.23	27	2.44	15.3	16	0.68	42	20	4124	0.64	0.29
1402.654	3173	61.27	27	2.40	17.5	16	2.42	43	20	4127	0.37	-1.80
1419.976	3213	61.33	28	2.41	16.9	16	1.76	45	19	4077	1.76	-1.26
1342.282	3037	62.01	28	2.40	17.3	16	2.16	30	29	4020	3.22	-1.56
1418.535	3209	62.58	29	2.44	15.2	15	0.64	45	19	4120	1.87	-0.23
1399.029	3165	63.36	30	2.44	14.8	16	0.51	42	20	4081	0.44	0.95
1428.613	3232	63.49	30	2.43	15.4		0.71	47	18	4168	0.55	
1343.017	3039	64.84	32	2.42	16.0	16	1.04	30	29	4020	1.87	0.43
1401.205	3170	64.98	32	2.44	15.0	15	0.59	43	20	4115	0.71	0.43

1393.954	3154	65.34	32	2.46	14.0	16	0.33	42	21	4139	0.79	1.86
1347.419	3048	65.54	32	2.47	13.5	15	0.24	32	28	4150	0.61	1.28
1403.377	3175	65.59	32	2.39	17.8	17	2.93	43	20	4102	0.29	-1.12
1378.814	3119	66.56	34	2.45	14.7	16	0.47	40	21	4093	0.61	1.08
1380.997	3124	67.18	34	2.43	15.6	17	0.83	40	21	4086	0.53	1.24
1348.882	3052	67.87	35	2.47	13.3	15	0.22	32	28	4166	0.84	1.37
1378.086	3118	68.37	36	2.48	12.8	15	0.16	40	22	4136	0.77	2.66
1343.752	3040	69.15	37	2.44	15.2	17	0.65	31	29	4043	1.25	1.32
1405.544	3180	69.69	37	2.47	13.5	15	0.24	43	20	4144	0.60	1.69
1423.578	3221	70.47	38	2.51	10.8	18	0.05	46	18	4145	0.39	7.52
1383.178	3129	70.47	38	2.50	11.4	14	0.07	40	21	4160	0.49	3.02
1391.779	3149	70.55	38	2.51	10.9	15	0.06	41	21	4226	0.79	3.91
1377.357	3116	71.21	39	2.48	12.5	16	0.14	40	22	4126	1.00	3.58
1414.934	3201	71.22	39	2.49	11.8	14	0.09	45	19	4250	0.63	2.14
1350.345	3055	71.43	39	2.50	11.6	14	0.08	33	27	4282	0.86	2.35
1406.267	3182	71.80	40	2.47	12.9	16	0.17	43	20	4231	0.65	2.59
1346.687	3047	71.92	40	2.51	10.7	14	0.05	32	28	4281	0.61	3.21
1420.696	3214	72.39	40	2.46	14.0	17	0.33	45	18	4074	1.00	3.23
1345.955	3045	72.63	41	2.51	11.0	14	0.06	31	28	4262	0.66	3.19
1408.434	3187	72.64	41	2.45	14.5	15	0.43	44	19	4049	1.36	0.68
1381.724	3126	72.86	41	2.45	14.3	16	0.39	40	21	4059	0.40	2.20
1351.809	3058	73.66	42	2.56	8.1	13	0.01	33	27	4437	0.38	4.79
1362.042	3082	73.67	42	2.49	11.8	14	0.09	36	24	4158	1.53	2.32
1382.451	3128	74.00	42	2.51	10.8	15	0.05	40	21	4166	0.46	4.66
1417.095	3206	74.73	43	2.51	11.0	16	0.06	45	19	4160	0.74	5.48
1390.326	3146	74.89	43	2.49	12.1	15	0.11	41	21	4194	0.72	2.92
1349.614	3053	74.96	43	2.52	10.4	14	0.04	33	27	4288	0.45	3.65
1411.325	3193	75.10	44	2.49	11.9	13	0.10	44	19	4208	1.55	1.59
1351.077	3057	75.21	44	2.53	9.4	14	0.02	33	27	4324	0.70	4.38
1404.099	3177	75.69	44	2.45	14.2	18	0.37	43	20	4004	0.35	3.89
1371.528	3103	77.44	46	2.49	11.9	15	0.10	39	22	4295	0.92	3.52
1363.503	3085	77.48	46	2.52	10.3	13	0.04	37	24	4310	1.57	3.07
1393.532	3153	77.86	47			16	0.00	42	21	4155	0.62	16.16
1421.417	3216	79.41	49	2.50	11.5	18	0.07	46	18	4118	0.73	6.20
1364.233	3086	79.45	49	2.51	10.6	14	0.04	37	24	4268	1.13	3.26
1376.628	3115	79.75	49	2.52	10.2	15	0.04	39	22	4353	0.77	4.37

1391.053	3147	79.81	49	2.50	11.2	16	0.06	41	21	4217	0.61	4.40
1393.229	3152	80.36	50	2.52	10.2	16	0.04	42	21	4197	0.51	5.53
1407.712	3185	80.69	50	2.47	12.9	16	0.17	44	19	4121	1.41	2.86
1344.487	3042	80.88	50	2.51	11.0	18	0.06	31	29	4043	0.89	6.73
1394.679	3155	82.15	52	2.51	10.8	17	0.05	42	21	4121	0.55	5.74
1383.905	3131	82.17	52	2.52	10.5	16	0.04	40	21	4185	0.72	5.36
1396.854	3160	82.60	52	2.50	11.7	17	0.09	42	20	4127	0.35	5.40
1389.6	3144	82.78	53	2.56	8.0	16	0.01	41	21	4314	0.50	7.63
1415.654	3203	82.90	53	2.47	13.1	16	0.20	45	19	4099	0.93	2.98
1362.773	3083	83.32	53	2.54	8.8	15	0.02	37	24	4228	0.97	5.97
1375.9	3113	83.37	53	2.55	8.5	14	0.01	39	22	4387	0.61	5.61
1370.8	3101	83.86	54	2.55	8.6	14	0.01	39	22	4341	0.19	5.41
1353.272	3062	85.47	56	2.54	9.2	16	0.02	34	27	4180	0.57	7.16
1375.171	3111	85.56	56	2.55	8.4	15	0.01	39	22	4321	0.61	6.25
1395.404	3157	87.60	58	2.53	9.5	16	0.02	42	21	4224	0.47	6.63
1374.443	3110	87.64	58	2.56	8.0	15	0.01	39	22	4303	0.43	7.28
1409.157	3188	88.11	59	2.51	11.0	16	0.06	44	19	4078	0.93	5.50
1352.541	3060	88.92	60	2.55	8.5	16	0.01	33	27	4242	0.82	7.22
1361.312	3080	89.18	60	2.55	8.3	17	0.01	36	25	4004	0.79	8.40
1372.257	3105	89.74	61	2.52	10.4	16	0.04	39	22	4065	1.11	5.25
1345.222	3043	90.49	61	2.54	9.2	17	0.02	31	28	4150	0.45	7.46
1410.602	3191	91.13	62	2.57	7.5	15	0.01	44	19	4287	0.66	7.81
1372.985	3106	91.89	63	2.52	10.3	18	0.04	39	23	4121	0.80	7.62
1412.047	3195	93.09	65	2.54	8.9	17	0.02	44	19	4198	0.91	8.15
1416.374	3204	93.88	65	2.53	9.8	17	0.03	45	19	4130	0.59	7.60
1367.154	3093	95.66	68	2.56	8.0	17	0.01	38	23	4106	0.10	9.35
1422.137	3218	96.14	68	2.51	10.8	20	0.05	46	18	4124	0.64	9.45
1422.857	3219	97.76	70	2.53	9.4	21	0.02	46	18	4089	0.42	11.49
1413.492	3198	98.95	71	2.56	7.7	16	0.01	45	19	4313	0.28	8.48
1373.714	3108	99.56	72	2.56	7.7	18	0.01	39	23	4098	0.39	10.13
1384.632	3133	99.68	72	2.55	8.2	18	0.01	41	21	4173	0.58	9.92
1364.963	3088	100.05	73	2.57	7.3	18	0.01	37	24	4226	0.74	10.21
1365.693	3090	101.12	74	2.59	6.1	18	0.00	37	23	4180	0.51	12.22
1406.989	3183	101.33	74	2.56	7.6	18	0.01	44	20	4139	0.38	10.20
1409.88	3190	102.29	75	2.57	7.2	17	0.01	44	19	4226	0.46	10.02
1414.213	3200	104.28	78	2.57	7.3	19	0.01	45	19	4111	0.65	11.56

1367.884	3095	105.26	79	2.57	7.3	19	0.01	38	23	4186	0.59	11.33
1385.359	3134	105.53	79	2.57	7.3	19	0.01	41	21	4150	0.48	11.68
1388.873	3142	105.96	80	2.59	6.2	19	0.00	41	21	4133	0.40	12.83
1354.004	3063	106.98	81	2.58	6.5	21	0.00	34	26	4087	0.54	13.99
1370.071	3100	107.74	82	2.58	6.5	20	0.00	39	22	3926	0.31	13.70
1357.661	3072	107.74	82	2.58	6.6	19	0.00	35	25	4023	0.36	12.45
1355.467	3067	108.55	83	2.58	6.4	20	0.00	34	26	4141	0.40	13.41
1386.086	3136	109.02	83	2.59	6.2	19	0.00	41	21	4126	0.40	12.54
1387.419	3139	109.81	84	2.58	6.3	19	0.00	41	21	4089	0.38	13.04
1368.614	3096	110.29	85	2.57	7.2	20	0.01	38	23	4162	0.44	12.65
1354.736	3065	110.66	85	2.59	6.3	21	0.00	34	26	4075	0.45	14.34
1358.391	3073	110.71	85	2.57	7.1	19	0.01	35	25	4117	0.65	12.17
1388.146	3141	111.36	86	2.58	6.8	21	0.01	41	21	4182	0.46	13.89
1386.692	3137	111.99	87	2.60	5.5	20	0.00	41	21	4151	0.40	14.20
1356.931	3070	112.14	87	2.57	7.0	21	0.01	35	26	4021	0.34	14.24
1366.424	3091	112.22	87	2.59	6.2	22	0.00	38	23	4099	0.53	15.63
1359.852	3077	112.52	87	2.56	7.6	21	0.01	36	25	4003	0.36	13.19
1412.77	3196	113.08	88	2.57	7.4	20	0.01	44	19	4050	0.66	12.79
1356.199	3068	113.87	89	2.57	7.0	21	0.01	35	26	4035	0.44	13.62
1360.582	3078	114.45	89	2.58	6.5	22	0.00	36	25	4014	0.45	15.74
1359.122	3075	115.58	91	2.56	7.7	21	0.01	35	25	3979	0.54	13.53
1369.342	3098	116.04	91	2.58	6.6	22	0.00	38	23	3981	0.30	15.70
1429.332	3234	65.17	32	2.45	14.1		0.35	47	18			
1430.051	3235	86.17	56	2.52	10.2		0.04	47	18			
1430.77	3237	90.77	62					47				

Appendix 2 :Example of compaction mechanism and the construction of synthetic seismogram (Glover, 2012)
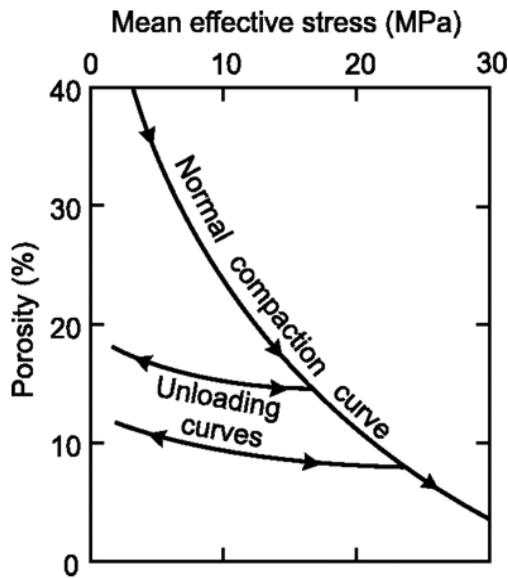

*Figure 1:*The normal compaction curve for a sediment follows a path of decreasing porosity with increasing mean effective stress. An unloading curve is associated with each point on the normal compaction curve and defines the poroelastic response of the sediment during unloading and reloading.
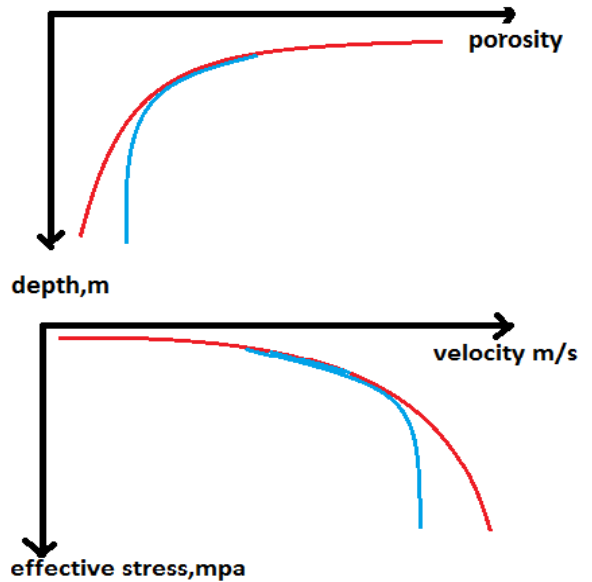

Figure 2 & 3 above show the example of unloading curve (blue line) compared to the normal compaction curve (red line).
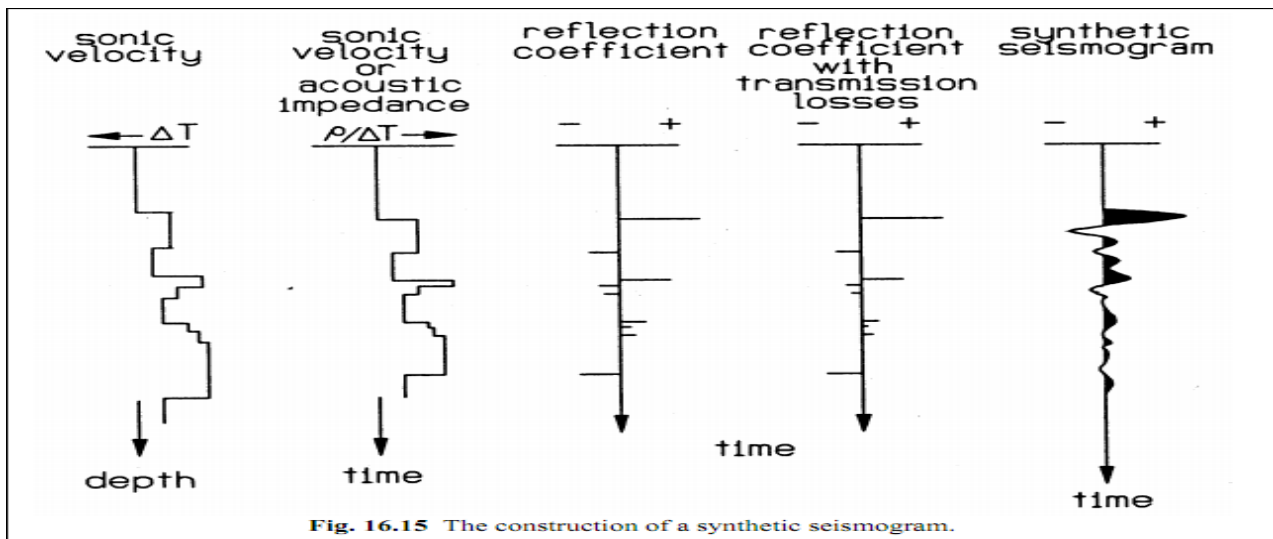

Fig. 16.15 The construction of a synthetic seismogram.

Appendix 3: Reference data for Wyllie's time average equation. (Glover, 2012)

Table 16.2 Values for Δt and V for use in Wyllie's time average equation.

Material	Δt (μs/ft.)	V (ft./s)	V (m/s)
Compact sandstone	55.6 – 51.3	18000 – 19500	5490 – 5950
Limestone	47.6 – 43.5	21000 – 23000	6400 – 7010
Dolomite	43.5 – 38.5	23000 – 26000	7010 – 7920
Anhydrite	50.0	20000	6096
Halite	66.7	15000	4572
Shale	170 – 60	5880 – 16660	1790 – 5805
Bituminous coal	140 – 100	7140 – 10000	2180 – 3050
Lignite	180 – 140	5560 – 7140	1690 – 2180
Casing	57.1	17500	5334
Water: 200,000 ppm, 15 psi	180.5	5540	1690
Water: 150,000 ppm, 15 psi	186.0	5380	1640
Water: 100,000 ppm, 15 psi	192.3	5200	1580
Oil	238	4200	1280
Methane, 15 psi	626	1600	490